Centre for Geo-Information

Thesis Report GIRS-2004-37

Multi-temporal analysis of vegetation characteristics in Central Brazil, using ASTER imagery

Fenny van Egmond

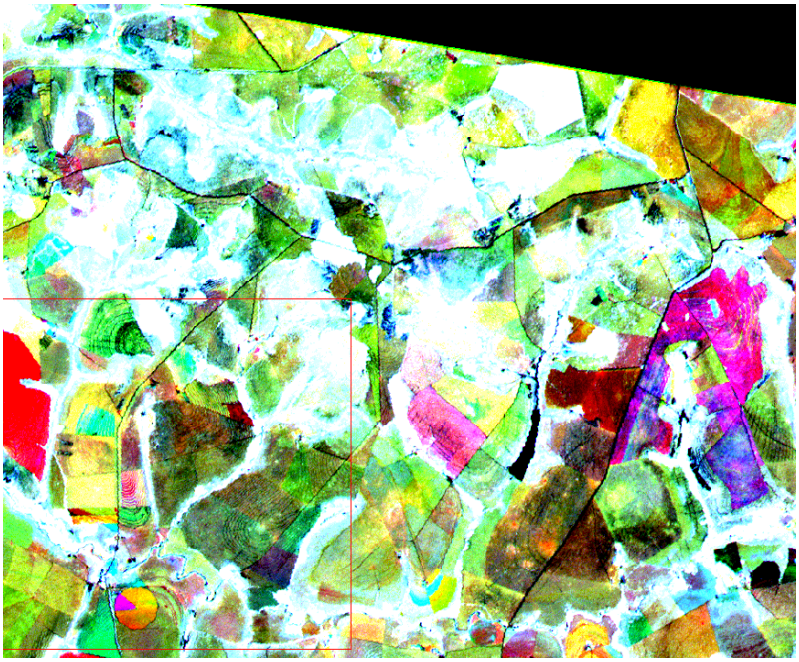

September 2004

WAGENINGEN UNIVERSITY
WAGENINGEN UR

Author: Fenny van Egmond
Haarweg 13
6709 PH Wageningen
e-mail: fenny_van_egmond@hotmail.com

Course code: K075-704 at Wageningen University (27 stp)

Thesis report code: GIRS-2004-37

Supervisors: G.F. Epema
A. Vrieling

For:

Wageningen University (WUR)
Laboratory of Geo-Information Science and Remote Sensing
Centre for Geo-information
Wageningen, the Netherlands

September 2004
Wageningen, The Netherlands

Abstract

Total vegetative ground cover is one of the most important factors in the protection of soil against erosion. Total vegetative ground cover includes green and yellow vegetation. The objective of this study is to estimate the annual cycle of total, green and yellow vegetative ground cover (VGC) in the Brazilian *cerrado* using a vegetation index derived from a series of seven Advanced Spaceborne Thermal Emission and Reflection Radiometer (ASTER) satellite images and field data of vegetative ground cover. Brazilian *cerrado* is very heterogeneous and consists of different mixtures of pasture, shrub and tree vegetation. A linear relation was derived between the Normalized Difference Vegetation Index (NDVI) and the field data of total and green VGC of both wet and dry season. From this relation total, green and yellow VGC maps could be constructed. These regression equations were interpolated for the other five ASTER images because large differences are found between wet and dry regression equations. A reasonable correlation between NDVI and total VGC in wet season was found (R^2 = 0.55), although the correlations for green VGC and in dry season (R^2 = 0.16-0.20) were poor. This enables an estimation of total VGC with an uncertainty of 15 % VGC. The decrease of VGC in dry season could be estimated but the actual yellowing of vegetation could not be detected significantly. Trend analysis indicates no seasonal dynamics of the original *cerradao* vegetation and large dynamics in areas with pasture and shrubs. Pasture is most sensitive to erosion and especially in the period from August to October when vegetative ground cover is low and precipitation can be intense.

Contents

1. Introduction

1.1 Context and background

Worldwide, soil erosion is a serious threat to sustainable agriculture. This has been recognised by among others Bennett (1939), Kilewe and Ulsaker (1984), Nill *et al.* (1996) and Laflen and Roose (1997). With a growing world population the demand for food increases. Therefore, more and more land is taken into cultivation, usually causing deforestation. In these new cultivated areas the natural equilibrium is disrupted. A way for nature to correct this equilibrium on hilly terrain is soil erosion. Soil erosion can be defined as the detachment and translocation of soil particles by moving water or wind from their original locations to new depositional areas (Laflen and Roose, 1997). Another possible agent of soil erosion is ice (Lal, 1990). Erosion reduces soil productivity through physical loss of topsoil, reduction in rooting depth, removal of plant nutrients and loss of water (Okoth, 2003). This soil loss leads to declining yields. Erosion research is therefore important for sustainable agriculture and land use planning.

Apart from the agents of soil erosion there are a number of factors that can stimulate the development or progression of soil erosion such as slope gradient, slope length, (canopy) cover or land use, climate, geology, soil properties, management, etc. (Okoth, 2003). The agents and erosion-controlling factors mentioned vary spatially and temporally. Therefore, the demand for an efficient and relatively cheap data-collection system that can deal with the spatial and temporal variability is high. In order to produce erosion risk maps a good estimate of the risks caused by the various erosion-controlling factors and agents is needed. One of these factors is the annual fluctuation in the vegetative ground cover (VGC) of the area. This fluctuation includes the variation of green and dry vegetation cover and bare soil. The research area of this study is located near Uberlândia in Central Brazil. This area is subject to various types of erosion, has a heterogeneous vegetation cover and a clear dry season that results in strong fluctuations of green and dry vegetative ground cover and bare soil. A technique to assess the spatial and temporal variability of this fluctuation of vegetative ground cover is remote sensing (Hashem *et al.*, 2000).

Remote sensing is the science and art of obtaining information about an object, area, or phenomenon through the analysis of data acquired by a device that is not in contact with the object, area or phenomenon under investigation (Lillesand and Kiefer, 2000). Nowadays, data gathered by remote sensing is usually in the form of satellite imagery or aerial photography. Remote sensing already supported erosion research in several projects, using imagery from SPOT (Carreiras *et al.*, 2002; Cyr *et al.*, 1995), IKONOS (Hashem et at., 2000), Landsat (Maldonado *et al.*, 2002; Seyler et al, 2002), ERS-2 SAR (Price *et al.*, 2002).

Remote sensing offers the ability to monitor temporal and spatial changes because of its ability to take snapshots of an area in time and thus of certain dynamics on the earth surface. It can provide data for a large area at the same time because of the high altitude of the sensor. It is able to provide various spectral and spatial resolutions depending on the satellite or aerial photography device. Furthermore it can give an account of and monitor important erosion-controlling factors,

like vegetative ground cover, slope gradient and slope length and to a certain extent the moisture content, the organic matter content, soil texture and surface roughness of soils. At the same time it provides rough information about the presence, species and condition of vegetation.

The vegetative ground cover can be studied using vegetation indices. A vegetation index is a formula that can be applied to a remote sensing image and is designed to separate the green vegetated area from the non-vegetated area. Although vegetation indices are usually designed to determine the amount of green vegetation present, this research will focus on the total VGC, so the green and the non-green vegetation. By studying the annual cycle of green and non-green VGC the erosion risk in the area can be spatially assessed by comparing the data to precipitation data. At the same time the annual spatial dynamics of VGC as a result of precipitation and management influences can be studied.

A lot of research has been done on the spectral behaviour of vegetation under stress using vegetation indices and Landsat or SPOT imagery (Cyr *et al.*, 1995; Baret and Guyot, 1991; Price *et al.*, 2002). Some research focuses on the amount of crop residue present or the yellowing of bushes and trees and its spectral behaviour (Biard and Baret, 1997; Bonn et al, 1997; Elvidge, 1990; Idso *et al.*, 1980). Tucker (1977) is able to distinguish dry standing biomass from wet standing biomass using the wavelength range of 0.35 to 0.44 μm. However, when studying the spectral behaviour of grass or *cerrado* vegetation, mainly research is described where hyperspectral imagery is available and a number of variations on the spectral unmixing technique are used (Roberts *et al.*, 1993; Asner et al, 2003; Hostert *et al.*, 2003). Research on the use of vegetation indices in studying photosynthetically active and non-active vegetation or grass without hyperspectral imagery and with a finer resolution than Landsat and SPOT is sparse (Rundquist, 2002; van Leeuwen and Huete, 1996; Ferreira *et al.*, 2003).

The advantages of ASTER (Advanced Spaceborne Thermal Emission and Reflection radiometer) are that it produces images with a wider spectral range and a higher spectral resolution than its predecessors do. ASTER provides satellite images with 15m (visible and near infrared spectral region), 30m (shortwave infrared spectral region), and 90m (thermal infrared spectral region) spatial resolutions.

The launch of ASTER provides new opportunities to get an estimate of the total, the green and yellow vegetative ground cover in heterogeneous areas such as the Brazilian *cerrado* biome using multi-spectral imagery and vegetation indices. A procedure that has encountered a lot of difficulties so far while the total vegetative ground cover is an important erosion-controlling factor and therefore valuable in erosion research.

1.2 Research questions

The main objective of this thesis research is to assess the spatial and temporal dynamics of vegetative ground cover in the Uberlândia area, Central Brazil, using optical satellite imagery. This includes green and non-green vegetation cover. ASTER imagery is used because of its high spectral and spatial resolutions in comparison with e.g. Landsat imagery.
The resulting research objectives can be described as:

- To derive the vegetative ground cover of the soil using a vegetation index on ASTER imagery, after summarizing the benefits and drawbacks of possible methods in the research area in Central-Brazil.
- To assess the annual dynamics and spatial variability of vegetative ground cover and compare the results with precipitation data and management effects.

1.3 Report structure

This report consists of seven chapters:

Chapter 1: An introduction to the objectives and the context of this research.
Chapter 2: General information about the research area in Uberlândia, Central Brazil.
Chapter 3: The methodology that is used during the research, divided in the preparation of the imagery and available data and the methodology to derive ground cover maps of the area, followed by a description of the procedure to analyse the spatial and temporal trends in the vegetative ground cover over a year.
Chapter 4: The results of this research are presented. The accuracy of the pre-processing of the imagery is given, as well as the results of the analysis of the procedure to derive the ground cover maps. The analysis of the spatial and temporal trends is displayed as well as the validation carried out on the results.
Chapter 5: The general results of the research are discussed and placed in the scientific context.
Chapter 6: The main conclusions of this research are drawn.
Chapter 7: Recommendations for further research and for improvements of the current methodology are given.

2. Research area

The research area is located within the Triângulo Mineiro, Minas Gerais, Central-Brazil, near the city of Uberlândia. The size of the area is about 10 by 10 km and the altitude ranges from 650 to 850 m above mean sea level.

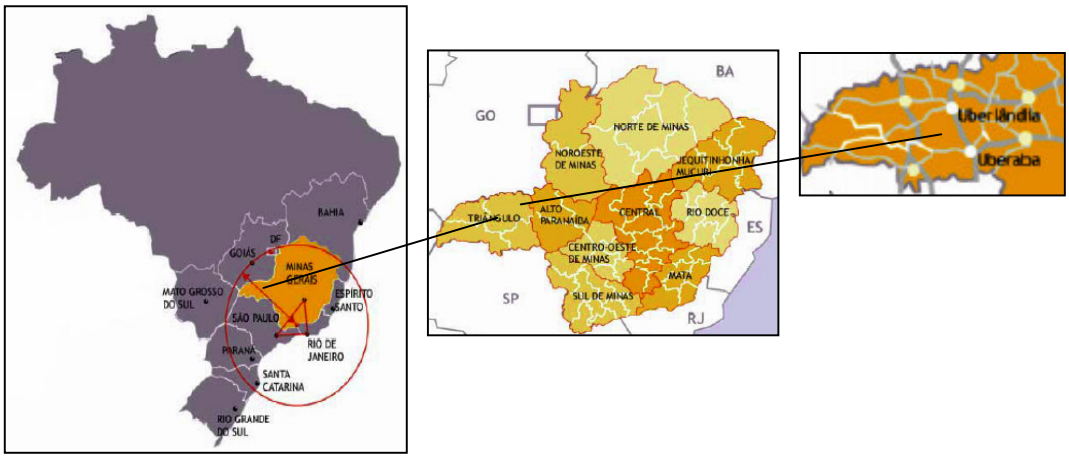

Figure 2.1. The research area (Hernandez, 2004)

The terrain is slightly undulating and weakly dissected with a medium inclination of 5-10 °. The area belongs to the sedimentary plateau region of central Brazil. The geology of the area has as base schist and quartzite from medium Precambrian covered by Mesozoic sediments from the Paraná Basin. Douradinho river cuts through sandstone and basalt from the Serra Geral Formation, arriving in the bottom of the valley to erode gneisses and granites of inferior Precambrian. Cenozoic sediments can be found at the tabulate plateaus and in residual relief, as well as covering structural terraces (Hernandez, 2004).

The soils of the area are mainly Red-Yellow Latosols. This is a soiltype in the Brazilian classification system that is comparable with the non-aquic Oxisols in the American USDA soil taxonomy classification system and Ferralsols in the FAO-classification system. The dominant chemical process in their formation is desilication (or ferralitization), leading to the nearly complete dissolution of weatherable minerals and the relative accumulation of stable secondary minerals in the clay fraction, particularly kaolinite, gibbsite, goethite ad hematite (Neufeldt *et al.*, 1999). The soils are very deep, very well drained, homogeneous and highly weathered and leached soils. They tend to have medium clay contents. They have low fertility and high acidity. When limed and fertilized, however, they become highly productive soils (Thomas and Ayarza, 1999). Other soils that are present in the area but less abundant are Podzols and Cambisols. Podzols are sandy, well drained poor soils. Their formation is governed by two processes, the process of cheluviation and chilluviation. The first captures the movement of soluble metal-

humus complexes (chelates) out of the surface layer to greater depth. The second is the subsequent accumulation of Al- and Fe-chelates in a spodic B-horizon. This means that most organic compounds are moved out of the surface layer causing a low chemical fertility. Cambisols are developing soils that have a medium to fine texture lacking specific features like illuviated clay, organic matter, aluminium and/or iron compounds. (Driessen and Dudal, 1991)

Figure 2.2 Ferralsol, Red Latosol in Brazilian classification system. (FAO, 2001)

The area has a humid tropical climate with a clear dry season and a precipitation of 1,500 mm/year (figure 2.3). The wet season extends from October to March with a higher intensity of precipitation from November to January (figure 2.3)(Baccaro, 1999; Ferreira and Huete, 2004). During dry season the air humidity reaches extremely low levels (less than 15 percent). The average annual temperature is 22 ºC, with a maximum in October and a minimum in July. (Thomas and Ayarza, 1999)

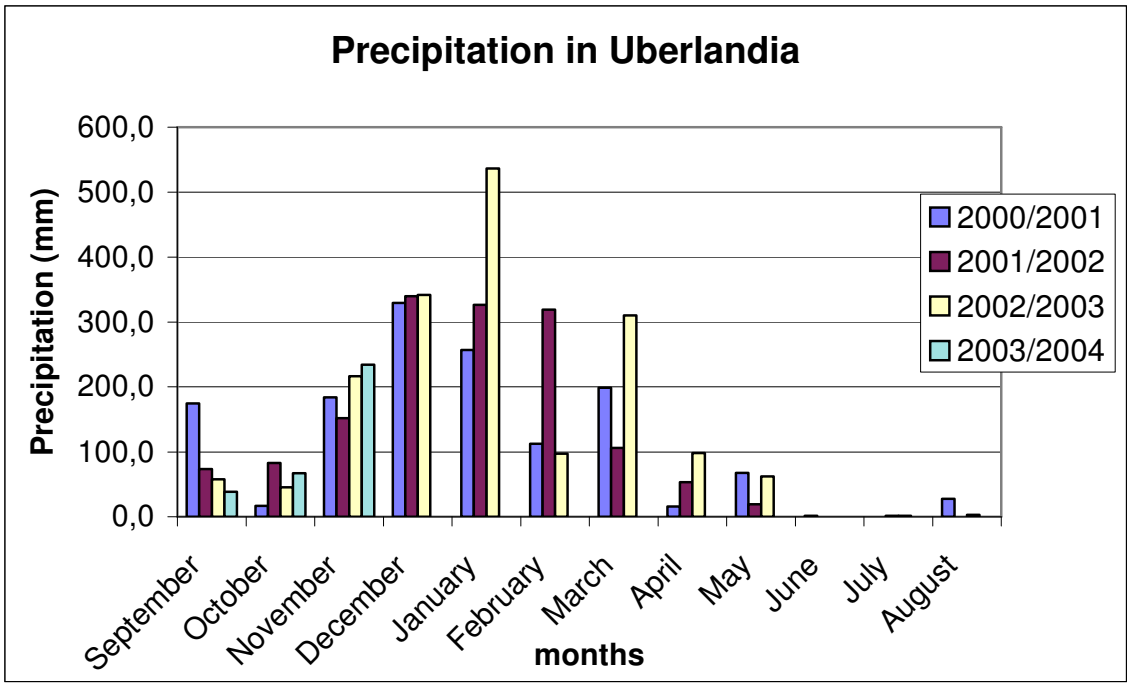

Figure 2.3 Precipitation measured at UFU- weather station, Uberlândia in the wet and dry seasons of 2000/2001 till 2003.

The original vegetation type is *cerrado*, which ranges from dense grasslands, usually with a sparse covering of shrubs and small trees, to almost closed woodland with a canopy height of 12-15 m (figure 2.4 and 2.5). However, in a large part of the research area it has been cut and transformed into pasture or agricultural fields with sugarcane, maize, soya and cassava. At some scattered locations *cerradao*, dense woodland, is still present. Along watercourses in the area there is *cerrado* woodland or gallery forest. The pasture and agricultural fields still bear some resemblance to the *cerrado* cover, since scattered trees and bushes are present in the fields. The population in the area is either living in the city of Uberlândia or on scattered farms throughout the research area.

Figure 2.4 *Cerrado* vegetation

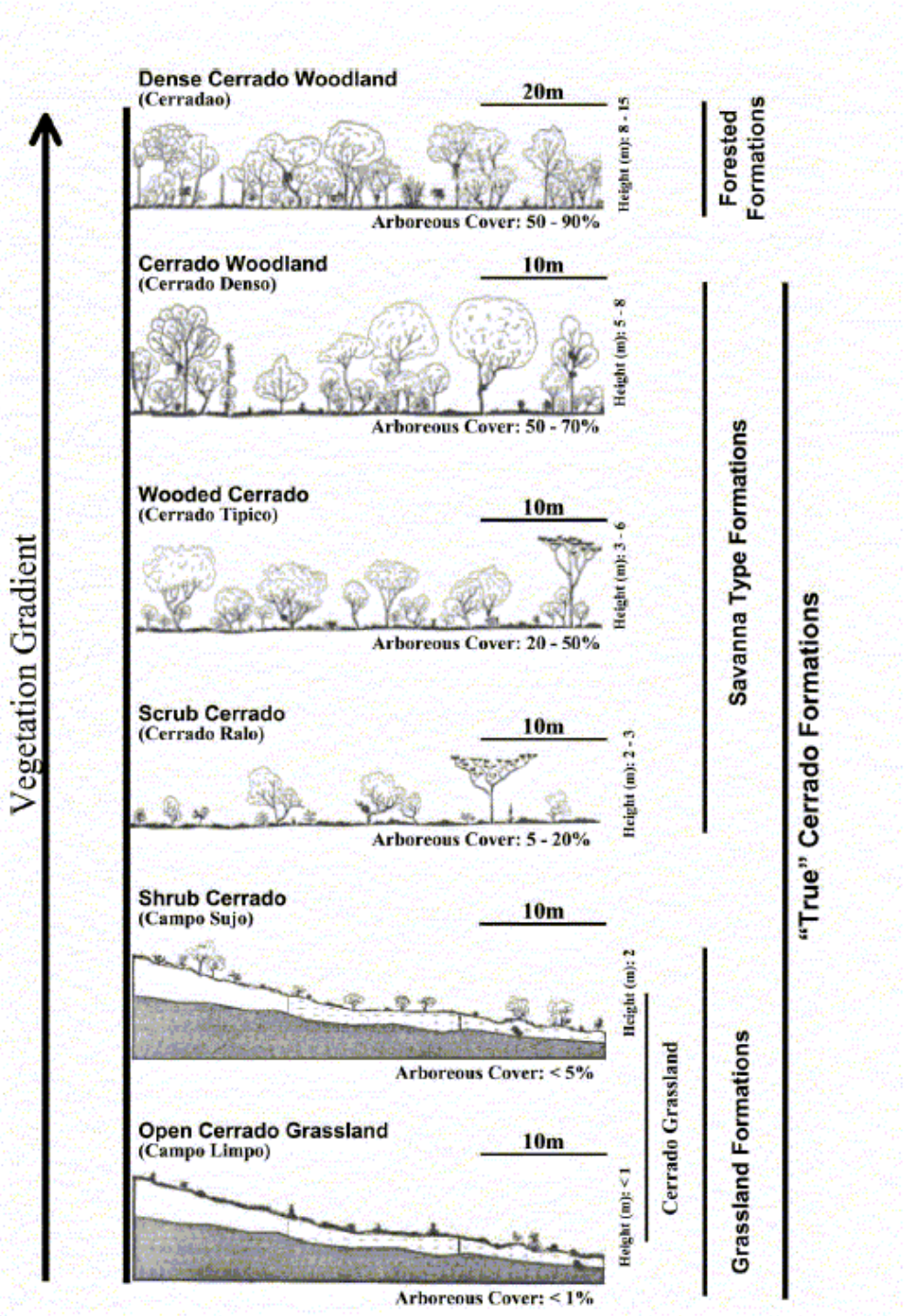

Figure 2.5 The different *cerrado* formations.

The pasture and agricultural fields in the region are degrading, among others because of sheet erosion and overgrazing, resulting in little ground cover and a further increase of sheet erosion. Also at agricultural fields soil erosion is a problem. Trying to limit soil erosion, contourbounds are created on the gently undulating fields. Contourbounds (figure 2.5) are small walls of earth of

about a meter high that are built perpendicular to the slope. The purpose is to decrease surface run-off and increase infiltration to protect the fields against sheet erosion.

Figure 2.5 Contour bounds in the research area.

The area has two specific erosion problems, sheet erosion (figure 2.6) and gully erosion (figure 2.7). Sheet erosion involves the removal of a uniform thin layer of soil by raindrop splash or water run-off, sometimes resulting in an extensive loss of rich topsoil. Raindrop action on bare soil disrupts aggregates, dislodges soil particles and compacts the erodible soil surface. If rainfall exceeds infiltration, a surface film of water forms, building up into flows of 2-3 mm deep. Continuing rainfall causes turbulence within the flow that may increase the water's erosive effect up to 200 times. Loss of the finest soil particles, to which the bulk of plant-available nutrients and organic matter adhere, affects the productivity of the land. Erosion may also result in removal of seeds or seedlings and reduce the soil's ability to store water for plants to draw upon between rainfall events. Soil deposited off-site through this type of erosion causes crop and pasture damage, water-quality deterioration and stream, dam, lake and reservoir sedimentation. (DNRE, 2004)

Figure 2.6 Sheet erosion

Gully erosion is the formation or extension of a channel or cut in the landscape that is sufficiently deep to not be routinely destroyed by tillage operations. Run-off water concentrated in rills or

depressions removes soil particles through sluicing - the washing effect of running water on loose grains. Material commonly moved is the size of fine to medium sand or may be derived from slaking, when large aggregates disintegrate upon wetting. Gullies may widen through lateral erosion, where water undercutting causes subsequent slumping of the sides. Gully sides may also be subject to splash, sheet or rill erosion. (DNRE, 2004)

Studies by Baccaro (1994) in Douradinho brook showed receding of the banks of the gully up to 3.00m between 1997 and 1998. The erosion incursions occur of walls due to a line of pipe flows. Underground caves develop, originating from the dynamics of the ground water causing seepage erosion. Such processes are promoting interfluvial dismantling because of receding headwaters as well as drainage caption. An inventory done by CEMIG (1995) found that of the active gullies number in Uberlândia municipality, 36 of them were located on the right part of Douradinho River. (Hernandez, 2004)

Figure 2.7 Gully erosion

Of the two erosion processes in the area, sheet erosion in the most important in the light of this research. Although gully erosion effects the total vegetative ground cover, the total vegetative ground cover effects sheet erosion. To reduce sheet erosion by guarding the vegetative ground cover all year round, the annual cycle of the total, the green and the yellow vegetative ground cover must be known. In this research this annual cycle is investigated.

3. Materials and Methods

3.1 Materials

In this study a serie of ASTER imagery, a Quickbird and a Landsat image are available. Added to the imagery, field data is present of two fieldwork periods together with precipitation data and a topographic map (table 3.1).

Table 3.1 Available data

Data	Date	Map projection	Datum	Format	Resolution	Viewing angle
ASTER	26 February 2001	UTM, zone 22S	WGS 84	Hdf	15 m	4
ASTER	9 Sept 2002	UTM, zone 22S	WGS 84	Hdf	15 m	4
ASTER	25 Febr 2003 (partly)	UTM, zone 22S	WGS 84	Hdf	15 m	1
ASTER	4 March 2003	UTM, zone 22S	WGS 84	Hdf	15 m	4
ASTER	23 May 2003	UTM, zone 22S	WGS 84	Hdf	15 m	5
ASTER	17 June 2003	UTM, zone 22S	WGS 84	Hdf	15 m	1
ASTER	24 June 2003	UTM, zone 22S	WGS 84	Hdf	15 m	4
ASTER	11 August 2003	UTM, zone 22S	WGS 84	Hdf	15 m	4
Quickbird	4 August 2003	UTM, zone 22S	WGS 84	Geo-tiff	0.6 m	
Landsat TM		UTM, zone 22	WGS 84	MrSid	28.5 m	
Topographic map of Fazenda Douradinho	1983	UTM/UTM22S	SAD-69/WGS 84	Jpg	-	
Overview-photographs	July and August 2002	Geograph. coor.	SAD-69	Jpg	-	
Nadir-photographs	July and August 2002	Geograph. coor.	SAD-69	Jpg	-	
Overview-photographs	December and January 2003/2004	Geograph. coor.	SAD-69	Jpg	-	
Nadir-photographs	December and January 2003/2004	Geograph. coor.	SAD-69	Jpg	-	
Field survey data	Dec-febr 2003/2004	UTM, zone 22S	SAD-69	xcl	GPS	
Precipitation data	1996 – 2003	At UFU				

ASTER was launched from Vandenberg Air Force Base in California, USA in 1999 aboard the Terra, which is one of the satellites in the EOS (Earth Observing System) Project. ASTER imagery is available in fourteen bands. All ASTER imagery in this research (table 3.1) is available at level 1B. Level 1B gives the radiance registered at the sensor. The imagery is geometrically and radiometrically corrected, but not ortho-rectified and not corrected for different

solar angles or the atmosphere. It gives the radiance at the top of the atmosphere. The radiances in digital numbers are therefore not directly comparable.

Late in the research period the same imagery became available at level 2B05. Therefore, level 2B05 imagery is only used for evaluating the results. Level 2B05 gives the reflectance at the earth surface. This level 2B05 imagery is geometrically and radiometrically corrected and corrected for atmospheric influences. It is not ortho-rectified.

Field data are available from two fieldwork periods, one in July/August 2002 and the other in December 2003 - February 2004. Geo-referenced photographs, overview photographs and photographs taken at nadir, are available of both periods. Of the second fieldwork period in the wet season of 2003/2004 over 360 geo-referenced sample points are taken that describe among others the type of vegetation cover and estimates of the percentage ground cover.

Precipitation data is available from a weather station in the neighbourhood of the research area. The data are daily and give a good estimate of the precipitation in the research area. (figure 2.3)

Table 3.2 Overview of the spectral bands of the available images

Spectral bands						
	ASTER		Landsat TM		Landsat ETM	
	Band nr.	(μm)	Band nr.	(μm)	Band nr.	(μm)
VNIR			1	0.45-0.52	1	0.45-0.52
Green	1	0.52-0.60	2	0.52-0.60	2	0.52-0.61
Red	2	0.62-0.69	3	0.63-0.69	3	0.63-0.69
Near-infrared	3	0.76-0.86	4	0.76-0.90	4	0.76-0.90
SWIR	4	1.60-1.70	5	1.55-1.75	5	1.55-1.75
	5	2.145-2.185	7	2.08-2.35	7	2.08-2.35
	6	2.185-2.225				
	7	2.235-2.285				
	8	2.295-2.365				
	9	2.360-2.430				
TIR	10	8.125-8.475				
	11	8.475-8.825				
	12	8.925-9.275				
	13	10.25-10.95	6	10.40-12.50	6	10.40-21.50
	14	10.95-11.65				

3.2 Pre-processing of imagery

The process of atmospheric and geometric correction is captured in a flowchart (figure 3.1).

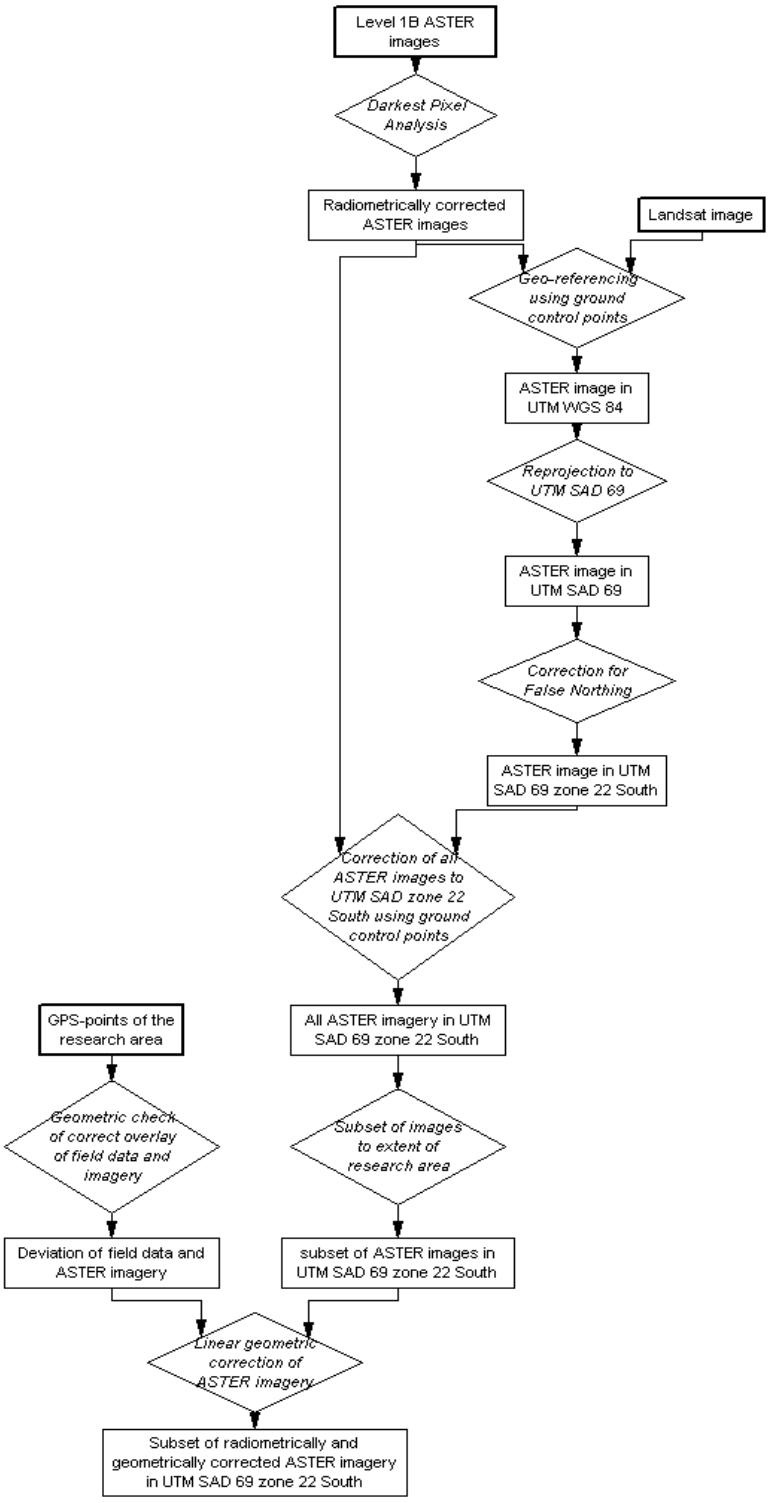

Figure 3.1 Flowchart of atmospheric and geometric correction of the ASTER imagery.

Since the images were taken at different dates and by different instruments and satellites, the solar angles, atmospheric conditions, viewing geometry and instrument response characteristics are different. Geometric distortion is caused by e.g. variations in altitude, velocity of the sensor platform, earth curvature, atmospheric defraction and relief displacement (Lillesand and Kiefer, 2000). This has to be taken into account during the analysis.

To correct for different atmospheric conditions at the different recording dates the Darkest Pixel Analysis is applied on the ASTER images (Schok and Clevers, 2001). It is assumed that there are some spots on the image with zero reflection. The lowest pixel values are supposed to be caused by atmospheric influence. Therefore, the lowest pixel value on each image per band is subtracted from all pixels in the image per band. This procedure is applied to the visible, near-infrared and middle-infrared bands on all images. The lowest pixel values that are subtracted can be found in Appendix A.

To overlay the various images, the images are geo-referenced, so the map projections, datum and spheroid are the same. The map projection is based on the datum, which refers to the spheroid used. All ASTER images have the same map projection and datum, but the other data has either a different map projection or a different datum. The topographic map and field data are all in SAD-69, so the ASTER data is transformed to this datum. All procedures are performed using ERDAS Imagine 8.5 software.

One of the images (11th August 2003) is geo-rectified using the ortho-rectified Landsat image using 65 ground control points that are identified on the screen. These are clearly recognisable points on both satellite images, e.g. crossroads, houses. The relative distribution of these points is used to derive a 1st order polynomial algorithm that can be applied to the entire image, thus creating a fit.

The datum of the Landsat image is WGS 84. The image is thus reprojected to SAD 69, zone 22 South and corrected for False Northing as the Landsat image has a False Northing. This means that 10.000.000 has been subtracted of the y-coordinates. To correct this we need to add 10.000.000 to the y-coordinates. The x-coordinates remain the same. The other ASTER images are transformed to the corrected ASTER image each using 55 ground control points. After the radiometric calibration and the geometrical correction the images are subsetted, to cut out the research area within each image. The extent of the Quickbird image was used.

Later in the research period more GPS ground control points became available. These GPS points are overlaid with the corrected imagery and a linear deviation of -41 m in the x-direction and 11 m in the y-direction was identified. The imagery is corrected, using 11 ground control points to create an optimal match with the field data.

3.3 Assessment of vegetative ground cover

3.3.1 Theoretical background of spectral methodology

Several procedures are available to separate bare soil and green and yellow vegetation. However, if differences between the spectral signatures of the three types of objects are missing, none of the methods can successfully differentiate between the objects. A spectral signature is the reflectance spectrum belonging to an object. A main problem is the distinction between yellowing vegetation and bare soil, because the two spectral signatures are very similar.

Theoretically, the largest differences between healthy and dry vegetation are in the red and near-infrared part of the spectrum. The difference between healthy and dry vegetation is the amount of chlorophyll and cartenoids present. Cartenoids have an absorption-peak between 300 and 500 nm and chlorophyll has an absorption-peak in the red (430 – 670 nm). This red-absorption of chlorophyll causes the green colour of healthy vegetation. In the same region the differentiation between bare soil and dry vegetation should be possible (figure 3.7). However, because the signatures are much alike bare soil can easily be mistaken for non-green vegetation and the other way around. Other possibilities are the detection of cellulose or lignin in the short wave infrared. Clouds and water have in contrast to green vegetation, larger visible reflectance than near-infrared reflectance. They are therefore easily distinguished from vegetation. (Lillesand and Kiefer, 2000)

The bands that prove to be able to make a distinct difference between bare soil and green and yellow vegetation can be used in either a vegetation index or in a spectral unmixing procedure. The two techniques are discussed in more detail.

There are three types of vegetation indices; ratio-based, orthogonal based and hybrid vegetation indices that are a mix of the first two types. Ratio indices use a ratio between the near-infrared and red reflectance or normalize the difference between them. Orthogonal based indices use the soil line in their calculation and assume that vegetation lines are orthogonal to the soil line and do not converge to one point as is assumed at ratio indices.

A major advantage of ratio index images is that they convey the spectral colour characteristics of image features, regardless of variations in scene illumination conditions. This enhanced discrimination is due to the fact that ratio-ed images clearly portray the variation in the slopes of the spectral reflectance curves between the two bands involved, regardless of the absolute reflectance values observed in the bands (Carlson and Riply, 1997). These slopes are typically quite different for various material types in certain bands of sensing. For example, the near-infrared-to-red ratio for healthy vegetation is normally very high. This is typically lower for stressed vegetation. (Lillesand and Kiefer, 2000)

Another technique to discriminate between bare soil, and different types of vegetation is spectral unmixing (Asner *et al.*, 2003; Roberts *et al.*, 1993; Borel *et al.*, 1994). This technique defines endmembers, spectral signatures of pixels with just one type of for example vegetation or bare

soil. These endmembers are the input of an algorithm that estimates the percentage of an endmember in a pixel, based on the spectral signature of the pixel, which is compared to the spectral signatures that are present in the library of endmembers previously defined. Since the research area is very heterogeneous in nature and no spectrometer data is available, spectral unmixing is not applied in this research because getting pure endmembers is very difficult in this case.

The technique that is used in this research with the before selected band combination is therefore a ratio vegetation index. Possible ratio-indices that are successful in literature are for example SACRI, SAVI and NDVI.

The Soil Adjusted Crop Residue Index (SACRI) (Bonn *et al.*, 1997) uses ASTER band 3 (near-infrared) and ASTER band 4 (short wave infrared). The formula is

$$SACRI = \frac{\alpha(\rho(NIR) - \alpha\rho(SWIR) - \beta)}{\rho(SWIR) + \alpha\rho(NIR) - \alpha\beta} \qquad \text{(equation 1)}$$

Where $\rho(NIR) = \alpha\rho(SWIR) + \beta$ is the bare soil line in the SWIR/NIR space. $\rho(NIR)$ and $\rho(SWIR)$ are the reflectances and α and β are the slope and intercept of the bare soil line. Benefits of SACRI are the sensitivity to low cover fractions. Disadvantages of this vegetation index are the saturation of the index after 25 % ground cover and necessity of the availability of a soil line.

The Soil-Adjusted Vegetation Index (SAVI) (Huete, 1988) is developed to account for changes of optical properties of the soil background and thus includes a soil-adjustment factor (L). It uses ASTER band 2 (red) and ASTER band 3 (near-infrared):

$$SAVI = \frac{\rho(NIR) - \rho(R)}{\rho(NIR) + \rho(R) + L}(1 + L) \qquad \text{(equation 2)}$$

Huete found the optimal value of L to vary with vegetation density. If no prior knowledge of vegetation amounts is present often 0.5 is used.

The Normalized Difference Vegetation index (NDVI) (Baret and Guyot, 1991; Ishiyama *et al.*, 1997; Zha *et al.*, 2003) uses TM bands 3 and 4, so ASTER bands 2 (red) and 3 (near-infrared). The formula is:

$$NDVI = \frac{\rho(NIR) - \rho(R)}{\rho(NIR) + \rho(R)} \qquad \text{(equation 3)}$$

Advantages of NDVI are its easy computation, its abilities to distinguish green vegetation and its widespread use in vegetation research with remote sensing. Disadvantages are the sensitivity to soil reflectance that increases errors at sites with sparse vegetation.
The index that is chosen for further analyses will have to be able to yield a workable relation between the percentage of ground cover and the results of the vegetation index. Furthermore, the index should be able to distinguish between the two processes of yellowing and decrease of the vegetative ground cover (VGC). These processes may look alike because they both lead to a decrease in chlorophyll absorption.

When an index is chosen the relation between the VGC and the vegetation index results is determined. These relations are expected to differ in wet and dry season. Apart from seasonal differences due to NDVI responses because of a decrease of photo-synthetically active vegetation due to decrease and yellowing of vegetation, Ferreira *et al.* (2003) found that different *cerrado* vegetation types (grass, wood and forest) show significant differences in the slope of biophysical relationships. They also found significant secondary influences in which the dry season biophysical relationships differ from the wet season relationships. Detectability of seasonal variations by NDVI also yielded differences between the vegetation types. Seasonal variations of grass (54 %) to forest (6 %) are detected as 29 % change (grass) to 12 % (forest). The field data of December 2003 - February 2004 include all *cerrado* vegetation types but the field data of July/ August 2002 only contain grassland with some shrubs. Van Leeuwen and Huete (1996) found a significant influence of litter on the performance of vegetation indices and NDVI in particular. They state that the composition of all above-ground plant components has to be known to make a reliable estimation of the ground cover.

3.3.2 Spectral properties

Whichever procedure is used to differentiate between green and yellow vegetative ground cover (VGC) and bare soil, if differences between the spectral signatures of the three types of objects are missing, none of the approaches can successfully differentiate between the objects. The bands of the signatures that show the largest differences between the objects are suitable to use in a vegetation index. If the objects show clearly distinct differences at a number of places in the spectrum spectral unmixing is a suitable technique to use. This is first judged using the spectral signatures of the objects. Then the selected bands are tested again by means of scatter plots to gain more insight in the differences between the feature spaces of the objects. The bands that show the largest spectral differences between the different objects are used in a vegetation index.

3.3.3 Vegetative ground cover estimation

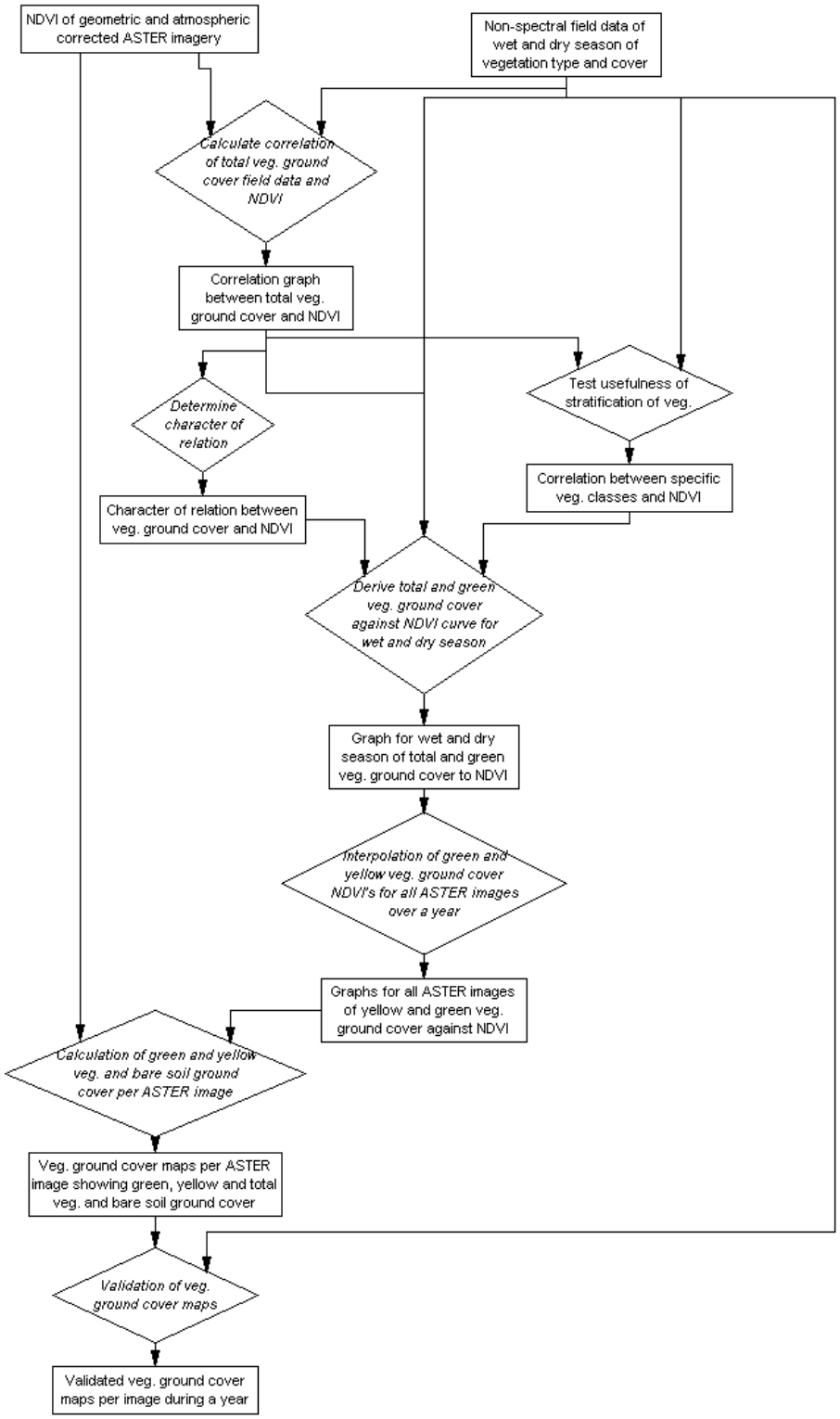

Figure 3.2 Flowchart the process of deriving and validating the vegetative ground cover maps of the series of seven ASTER images.

The bands that prove to be able to make a distinct difference between bare soil and green and yellow vegetation are used in either a vegetation index or in a spectral unmixing procedure. After listing the pro's and con's of the two techniques (chapter 3.3.1) it is decided that the technique that is used with the before selected band combination is a ratio vegetation index. Possible indices that are successful in literature are for example SACRI, SAVI and NDVI.

The index that is chosen for further analyses will have to be able to yield a workable relation between the percentage of ground cover and the results of the vegetation index. Furthermore, the index should be able to distinguish between the two processes of yellowing and decrease of the vegetative ground cover (VGC). These processes may look alike because they both lead to a decrease in chlorophyll absorption.

When an index is chosen the relation between the VGC and the vegetation index results has to be determined. Possible types of relations are for example linear or 2nd order polynomial. This relation is determined using the field data of December 2003 - February 2004 and the ASTER image of 4th March 2003. This combination is chosen because they are both more or less acquired in wet season although there is a time lap of at least nine months between image date and fieldwork period and 360 field data points are available. The dry season field data of July/August 2002 are related to the image of 9th September 2002 to observe possible differences in the relation between vegetation index and VGC in wet and dry season.

To compensate for all seasonal influences on the relation between VGC and the vegetation index, the wet and dry season correlation curves are used to calculate intermediate curves for the remaining images. Since no intermediate field data is available and there are no other seasonal changes than the transition from wet to dry season linear interpolation is applied to derive the intermediate correlation curves.

If necessary stratification can be applied to separate for example trees, shrubs and pasture according to field data to increase the accuracy of the estimation of the percentage ground cover. Although for example NDVI is known to be sensitive to soil brightness especially if different soil types are present (Elmore *et al.*, 2000; Huete, 1985), a stratification to soil or geology is probably not useful because the soils in the area all belong to the same major grouping of soils (EMBRAPA, 1982) and are therefore likely to have the same type of topsoil. More detailed information about differences within the major soil grouping is not available.

The results are validated using the ground cover map of 25th February 2003 and 4th March 2003 and the field data of December 2003 - February 2004. The purpose of the validation is on the one hand to get an indication of the accuracy of the VGC-estimate compared to the field data and on the other hand to get an indication of the uncertainty in the VGC-estimate that is caused by using the ASTER image of 4th March 2003 for the derivation of the wet season curve.

To obtain the first indication, a subset of 79 points of the field data set of 255 points is overlayed with the total, green and yellow VGC and bare soil map of 4th March 2003, the same image that

was used to obtain the wet season relation between NDVI and VGC, and the VGC maps of 25th February 2003. The difference between the VGC-estimate and the actual field VGC at the 79 points is calculated. This yields a systematic mean difference and a standard deviation of the difference between the actual and estimated VGC, the first being an indication of accuracy and the second an indication of uncertainty of the accuracy.

The second indication, the uncertainty in the VGC-estimate that is caused by using the ASTER image of 4th March 2003 for the derivation of the wet season curve, is obtained by subtracting the VGC maps of total, green and yellow vegetation of 25th February 2003 from the maps of 4th March 2003. The maps are derived with the same NDVI-VGC relations so differences are due to different NDVI values. Since the field data are collected in December to February, the field data set should be applicable to both images. Both calculations are executed for level 1B (top of the atmosphere radiance) and level 2B05 (surface reflectance) ASTER imagery.

Finally the VGC maps of 26th February 2001 are subtracted from the VGC maps of 4th March 2003 to obtain an indication of the uncertainty in the VGC-estimate that is due to the difference in time between the field data and the date of capture of the imagery. In the case of the 2003 maps this difference is one year, in the case of the 26th February 2001 maps, this time-difference is three years.

3.4 Spatial and temporal analysis of ground cover

This research question can be separated in two parts, spatial and temporal trends. Spatial trends that are expected are for example more degradation near the roads and less degradation near the river. Temporal trends that are expected are an increase in yellow vegetation in the course of the dry season as well as a possible decrease of the total vegetative ground cover (VGC).

The temporal trends are analysed by studying the statistics of the entire total, green and yellow VGC maps as well as the statistics of area's of interest of the three main vegetation types, forest, pasture and shrubs and pasture on each of the maps. To obtain an indication of the dependence of the results of the trend analysis on the quality of the imagery, it is carried out for the level 1B and level 2B05 ASTER imagery. The main trends and deviations are acknowledged and explained by the different vegetation types and precipitation data. If not sufficient, spatial analysis of the imagery will provide explanations. They are likely to include recent changes of land use, of resowing pasture areas or other land management measures or degradation effects. Differences between the two levels of imagery are noted and explained.

To get an indication of the difference between visible green vegetation and photo-synthetically active vegetation, the green and yellow as well as the photo-synthetically active vegetation throughout the year and the green looking but non-photo-synthetically active vegetation is calculated. This is done by applying the wet season green VGC correlation curve to all imagery.

4. Results and discussion

4.1 Accuracy of pre-processing of imagery

The Darkest Pixel Analysis is applied to the imagery to correct for atmospheric influences. The basic assumption of the analysis is that there are pixels in the image with zero reflection. This zero reflectance is usually caused by deep and clear water. Although water is present in the research area, the clearness turned out to differ throughout the year. Besides, the number and type of lakes and rivers turned out to be different throughout the imagery because of the different positioning of the research area on the images due to different viewing angles of the satellite, yielding a different snapshot of the surroundings. Although not entirely accurate, the analysis has removed some of the atmospheric influence in the imagery.

The Darkest Pixel Analysis is a linear correction and a review of the histograms of the images show only few differences in shape, either with or without the correction. The correction has no influence on the relations of the radiance digital numbers of the images relative to each other and hardly on the bands per image relative to each other.

When calculating the NDVI of the images part of the images contained negative NDVI values. To check if the negative NDVI values are due to the lack of extensive atmospheric correction the atmospherically corrected level 2B05 ASTER images are analysed. The histograms proved to have more or less the same shape but the bands shifted relative to each other, resulting is a higher NDVI and no more negative NDVI values

The accuracy of the geometric correction can be split in the different steps in the procedure. The accuracy of the different steps is depicted in table 4.1.

Table 4.1 Accuracy of geometric corrections, remaining deviation between ground control points of reference and input images

Operation	Nr. of image ground control points used	Control point error (m) of reference and input imagery
11th Aug '03 ASTER image to Landsat	50	39.1
9th Sept '02 to 11th Aug '03	55	7.5
4th March '03 to 11th Aug '03	55	8.0
23rd May '03 to 11th Aug '03	55	6.7
17th June '03 to 11th Aug '03	55	7.6
24th June '03 to 11th Aug '03	55	6.6

The accuracy of the correction procedures (table 4.1) is relative to each other. The accuracy of the correction of the ASTER image of 18th August 2003 to the Landsat image is relatively low, over one pixel of 28.5 m. The accuracy of the ASTER correction is less than one pixel of 15 m.

The systematic deviation of the corrected ASTER imagery from the GPS-points that became available in the course of the research was 41 m in the x-direction and 11.7 in the y-direction. After the linear correction of the ASTER imagery to the GPS-coordinates the systematic deviation of the imagery from the GPS-points is 0 m in the x-direction and 0.727 m in the y-direction. This does not include the accuracy of the GPS used, which on average is 5 to 10 m.

4.2 Spectral properties of vegetative ground cover and bare soil

The spectral signatures of the imagery divide roughly into wet season (October – March) and dry season (April – September) signatures with a transition zone in between. Therefore only two spectral signature or scatter plots are plotted. The signatures of May and start of June are intermediate. The locations for determining yellow and green vegetation and bare soil signatures are selected using the nadir-photographs of July/ August 2002. The photos are taken in dry season so the plotted signatures for yellow vegetation may actually correspond to a green vegetative ground cover. The bare soil spots remain bare all year round.

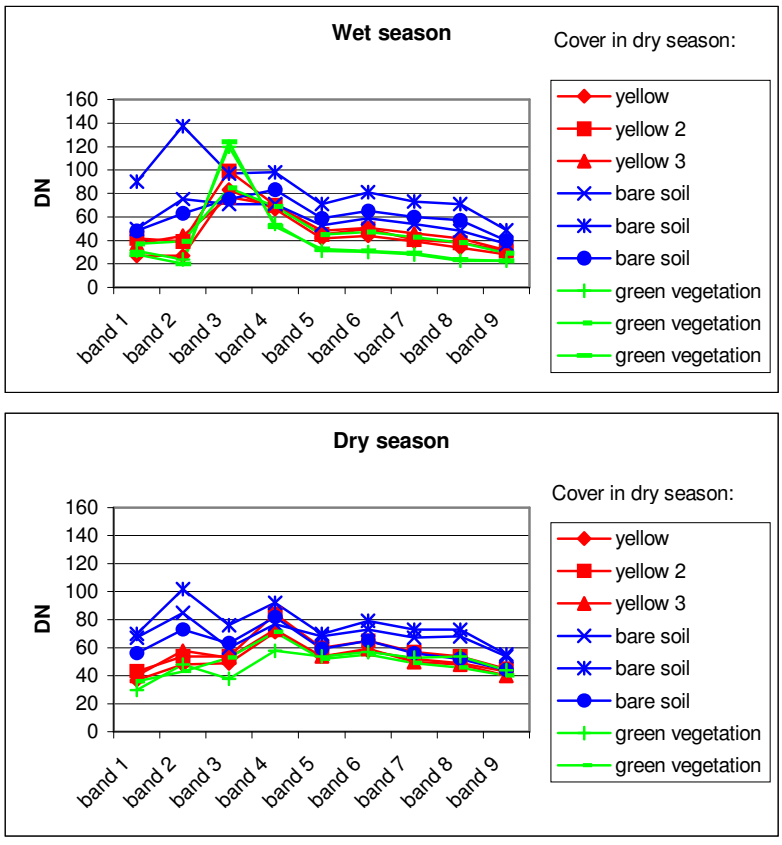

Figure 4.1 Radiance in Digital Numbers of various objects for various ASTER bands (dates: upper; 4 March 2003, lower; 11 August 2003) derived of ground truth August 2002. The images (level 1B, top of the atmosphere radiance) cannot be compared directly because of differences in incoming radiation throughout the year as a function of solar zenith angle and atmospheric condition.

In wet season the bare soil, green and yellow vegetation signatures are as expected, that is, the green vegetation shows a red edge; a high near-infrared reflection compared to a low red

reflection, while yellow vegetation and bare soil are more fluent and yellow vegetation reflection is lower than bare soil reflection (figure 4.2). In August (dry season) distinct differences between green and yellow vegetation and bare soil are hardly noticeable. The absorption of radiance by chlorophyll in green vegetation has declined, due to decreasing vegetation or yellowing of the vegetation as well as the absorption of radiance by water. The bands that are most promising because they show the largest differences are band 1 to 4. The differences in the short wave infrared are too small to distinguish between the different groups.

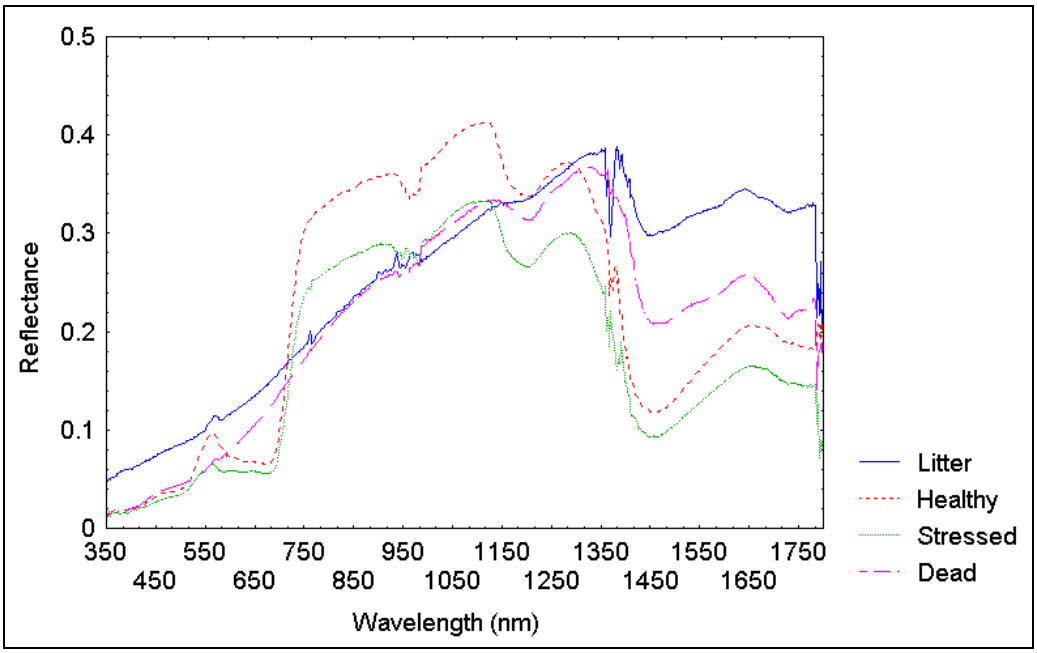

Figure 4.2, Bare soil, dry and green grass spectra (de Jong, 2004)

In figure 4.3 scatterplots between band 2 (red) and 1 (green) are shown. See Appendices for other plots.

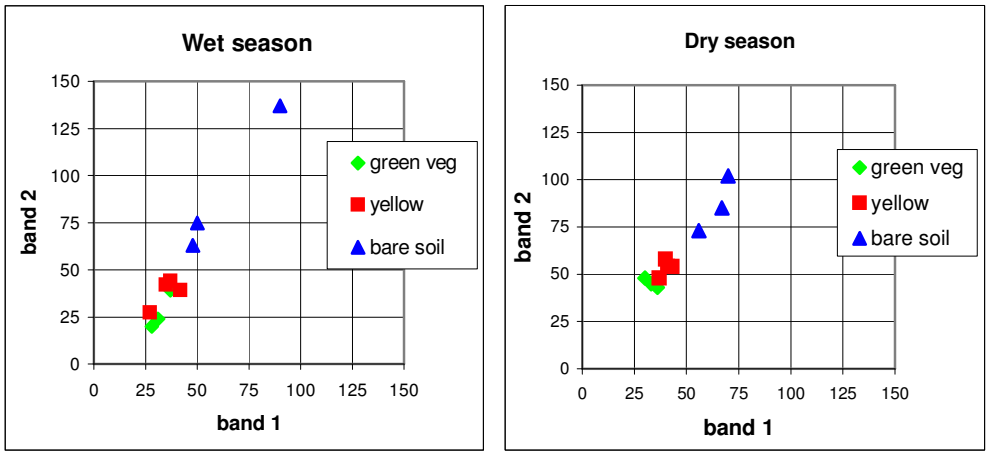

Figure 4.3 Scatterplots of band 2 with band 1 in Digital numbers (dates: left: 4 March 2003, right: 11 August 2003). Locations and labelling are chosen using ground truth of July and August 2002.

In both images vegetation can be separated from bare soil because the band 1 and band 2 reflectance of bare soil is higher than that of vegetation. In dry season the green and the yellow vegetation reflectance in band 2 is slightly higher and therefore slightly separable but also look like a mixture of green vegetation and bare soil. However, because ground truth was collected in dry season (July/August 2002) we know that the yellow vegetation points do represent yellow vegetation. It is not known how these locations look like in wet season. Because the green and yellow vegetation points are mixed, the yellow vegetation locations were probably green in wet season (October – March).

In further analysis the band 1 (green) will not be used for four reasons. Aerosols in the atmosphere influence the digital numbers of the green band, which causes more noise in the reflectance signal. The near-infrared and green bands are somewhat correlated for green vegetation spectra, to avoid this correlation it is better to use the red band instead of the green band. In literature usually the red and near-infrared band are used, which favours the use of the same bands in this study to enable comparison to other research results. Furthermore the behaviour of the digital numbers in the green and the red band is comparable.

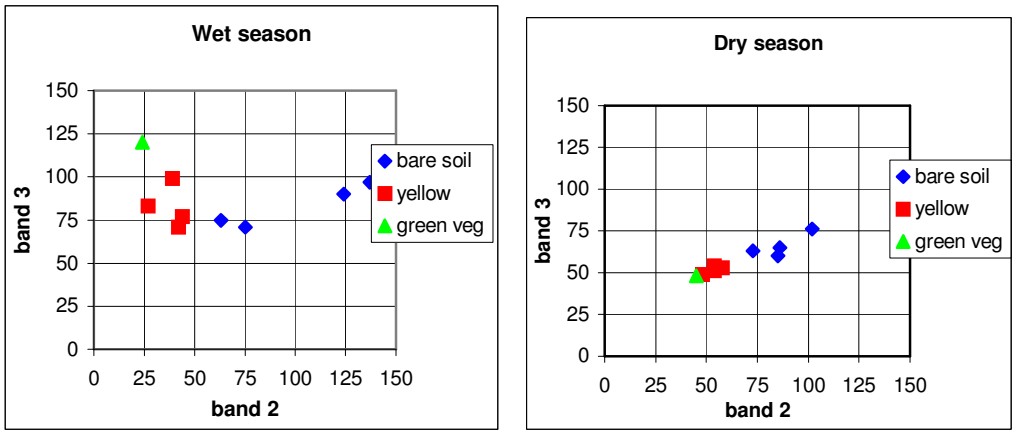

Figure 4.4 Scatterplots of band 3 with band 2 digital numbers (dates: left in wet season; 4 March 2003, right in dry season; 11 August 2003). Locations are chosen using ground truth of July and August 2002.

In wet season vegetation as a whole is separable from bare soil using ASTER band 2 (red) and 3 (near-infrared) (figure 4.4) because the points have a different orientation than the bare soil points. The band 2 reflectance is typically lower while the band 3 reflectance is higher for vegetation than for bare soil. The yellow vegetation points behave spectrally like green vegetation points as they are on a line perpendicular to the soil line. In dry season the vegetation and the bare soil points are more or less on a straight line. This drop in reflection in band 3 is caused by the yellowing of vegetation. It cannot be caused by a decrease of vegetation since the locations chosen had a full yellow vegetation cover in dry season.

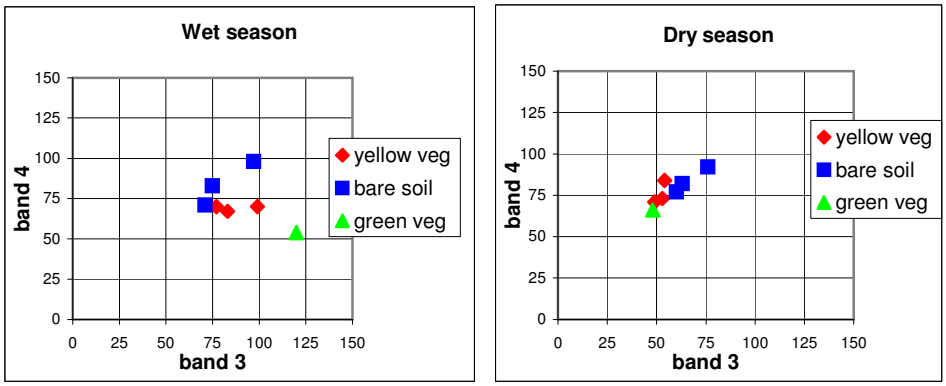

Figure 4.5 Scatterplots of band 4 with band 3 (dates: upper two in wet season; 4 March 2003, 26 February 2001, lower two in dry season; 11 August 2003, 9 September 2002). Locations are chosen using ground truth of July and August 2002.

Distinction between green and yellow vegetation and bare soil is only possible in wet season using ASTER band 3 (near-infrared) and 4 (Short wave infrared) since the reflactance is higher in band 4 for bare soil than for vegetation (figure 4.5). In dry season they cannot be separated using band 4 since there are no distinct differences in reflection in band 4 between vegetation and bare soil. Reflection in band 4 by vegetation is dependent on water absorption by the vegetation.

Concluding, ASTER band 2 and 3 are most suitable to use in this research. SACRI, SAVI and NDVI are optional vegetation indices. However, SACRI uses band 4, which was just ruled not suitable and as SACRI operates mainly at cover percentages below 25, SACRI is an unlikely choice. SAVI uses a soil-adjustment factor that is dependent on vegetation density (Huete, 1988). Since the vegetation density is not known beforehand, the purpose of this research is to determine the vegetation density, SAVI is an unlikely choice too. Therefore, the NDVI using ASTER band 2 (red) and 3 (near-infrared) is chosen in this research to assess the possibilities of estimating the total vegetative ground cover using a vegetation index and multispectal imagery, aided with field data.

4.3 NDVI and vegetative ground cover estimation

To examine the possibilities of the NDVI in assessing the total vegetative ground cover using ASTER imagery and field data (figure 3.2), NDVI curves are derived from all available images and compared to field survey data collected in December 2003 to February 2004. A number of locations have been selected all having pasture or degraded pasture as vegetation type and with ascending total vegetative ground cover (VGC) percentages. Because the field cover percentages of December to February are used, they merely indicate a trend in increasing vegetation. At the end of wet season the actual VGC will be higher than the percentage indicated in figure 4.6 since precipitation in wet season causes an increase in vegetation, while at the end of dry season the actual percentage will be lower than the percentage indicated in figure 4.6.

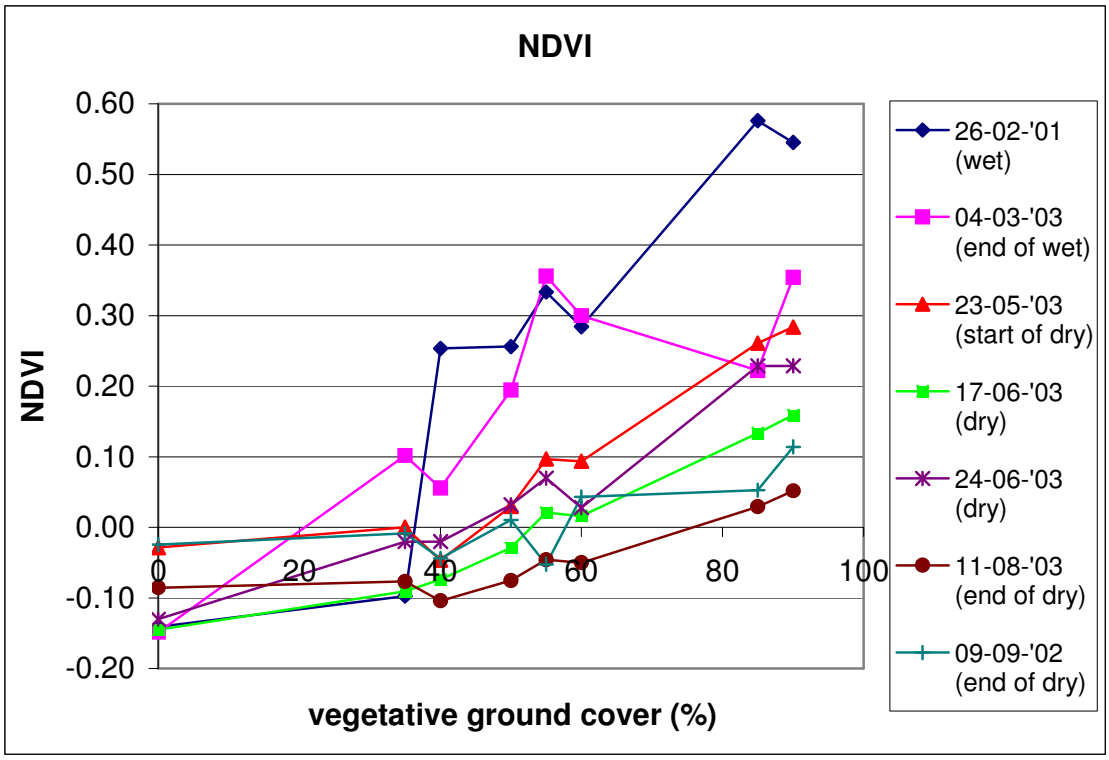

Figure 4.6, NDVI curve (band 3 and 2) of the digital numbers of all images/dates. The ground cover data are valid for December to February, since the ground truth used was taken in December 2003 to February 2004.

There are two trends between NDVI and VGC (figure 4.6), one the one hand the rise of NDVI with rising VGC and on the other hand the decrease of NDVI with steady VGC in the course of dry season. These two trends indicate that there are two processes active in the area that are important to this research, the yellowing of the VGC, the decrease of NDVI with steady total VGC in the course of dry season and the decrease and increase of total VGC, the increase of NDVI with increasing VGC. Although the VGC values of figure 4.6 are derived from field data in wet season (December 2003 – February 2004), field photos in dry season (July/August 2002) show that the decrease of total VGC is not as high as indicated by the drop in NDVI shown in figure 4.6. It is therefore possible to conclude that the NDVI drop in eth course of wet season is caused by yellowing of the VGC. However, it does indicate that confusion between the yellowing and decrease of VGC is likely. The differences between the curves of March and February are due to annual differences as are the differences between the curve of August and September.

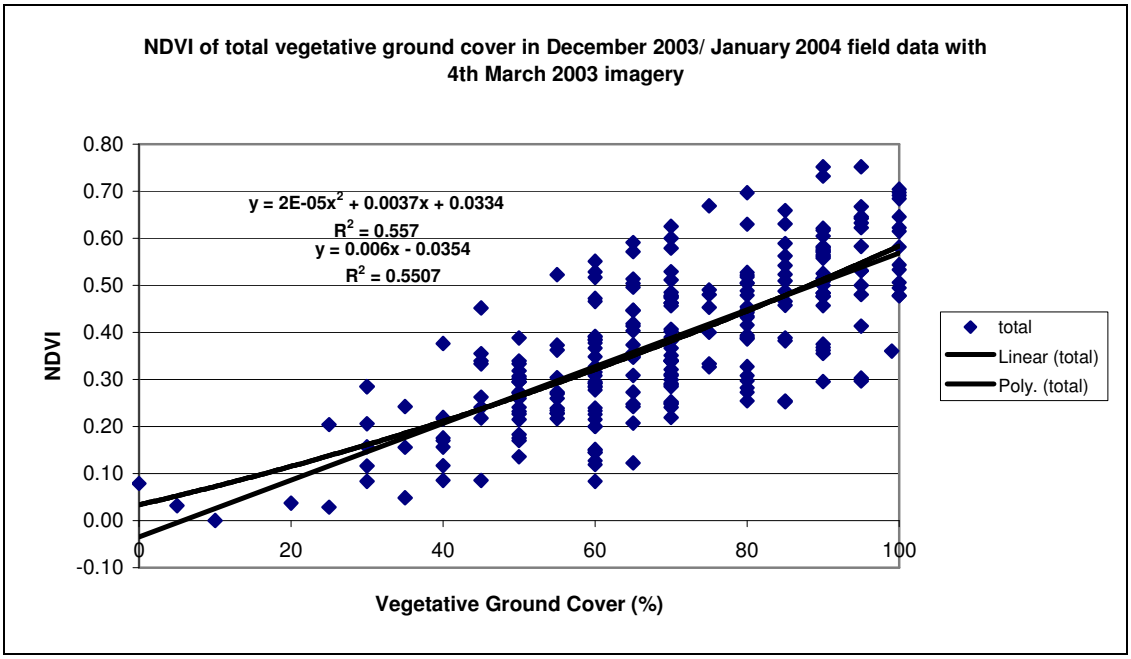

Figure 4.7 Testing of the type of relation between vegetative ground cover and NDVI results

Figure 4.7 is the result of all field data, except outliers that have been removed such as roads, water, buildings, agricultural crops and recently changed land use, plotted against the NDVI values that are derived from the ASTER image of 4th March 2003. Since the field work of December 2003 – February 2004 was conducted during this research more field data was available for figure 4.7 than for figure 4.6. A 2nd order polynomial trend line and a linear trend line are fitted through the data. The linear trend line has the best fit and the polynomial trend does not have surplus value compared to the linear trend. Therefore a linear relation between total VGC and NDVI is assumed. This is consistent with the relation between LAI, fractional vegetation cover and NDVI found in literature (Gao *et al.*, 2000), where the graph is linear up to a LAI of 1 and up to 100 % fractional cover (Carlson and Riply, 1997) and behaves asymptotically at higher LAI. Rundquist (2002) also found a strong linear relationship between green vegetation fraction (GVF) and NDVI response during growing season in native tallgrass prairie in Kansas (R^2 between .89 and .70 with R^2 dropping late in the growing season), and Zha *et al.* (2003) found a linear relation (R^2 = 0.74) between standardized NDVI and semiarid grassland in China. However, when senescent vegetation is studied using vegetation indices low R^2 (R^2 = 0.35) values are found (Cyr *et al.,*1995) and it is necessary to separate data from the senescence period form data from the growing phase.

The use of stratification to vegetation types is tested to try to improve the NDVI – VGC relationship. The results (table 4.2) show that although the R^2 for pasture is higher than the general R^2 the other R^2's are lower or are based on little observations. Therefore stratification to vegetation types does not increase the quality of the total VGC maps that estimate the total VGC of all vegetation types, or *cerrado* stages. Since the purpose is to get a VGC estimate of the entire research area the total vegetation relation between VGC and NDVI is used in the calculation of the VGC maps.

Table 4.2 R^2 of linear functions fitted through the graph of vegetative ground cover of December 2003 - February 2004 and the NDVI of the ASTER image of 4th March 2003.

NDVI-4th March 2003 ASTER image - December 2003/ February 2004 field data		R^2	Nr. of points used in estimation
Total vegetation	total	0.5507	255
	green	0.1880	76
Pasture	total	0.5745	79
	green	0.3679	18
Pasture and shrubs	total	0.3860	127
	green	0.0405	53
Cerrado	total	0.5143	37
	green	0.0145	8
Crops	total	0.7579	12
	green		

Now the correlation between total vegetation and NDVI in wet season has been found, correlation curves can be derived for total and green vegetation for wet and for dry season (figure 4.8). Field data is present that estimates total and green VGC. The correlation between total VGC and NDVI and the correlation between green VGC and NDVI is derived for both wet and dry season is derived by plotting the NDVI against field data of the two seasons, like in figure 4.7. Since the field data provided total and green VGC and not yellow VGC, the yellow VGC – NDVI relation is derived by subtracting the green VGC relation with NDVI of the relation of total VGC with NDVI. By subtracting the total VGC relation with NDVI from 100 we obtain a bare soil relation with NDVI.

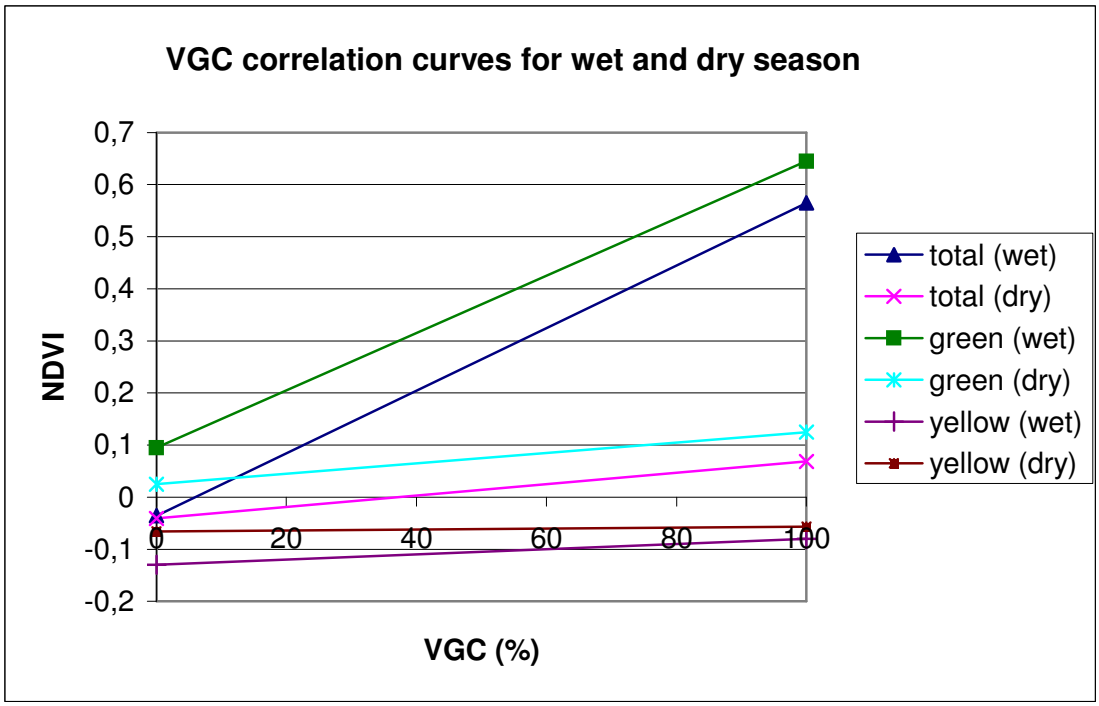

Figure 4.8 Correlation curves for wet and dry season using ASTER level 1B imagery and field data of December 2003 – February 2004 and July/August 2002. The total wet season curve is copied from the linear trend line of figure 4.7.

The differences between the wet season and dry season curves of total and green VGC have a few causes. It is probably caused by an increase in background brightness due to more litter in dry season (van Leeuwen and Huete, 1996) and by the different seasonal change response of grass, shrubs and forest (Ferreira and Huete, 2004). Since the different formations of *cerrado* have their own mixture of these components, this results in a different seasonal response causing a different NDVI – VGC relation for each *cerrado* formation in each season and causing net differences in overall total and green NDVI-VGC relations. Other causes are differences in solar illumination, viewing angles (Galvão *et al.*, 2004) and scaling of the images. Furthermore, these curves are derived for visible green and yellow vegetation, not for photosynthetic and non-photosynthetic vegetation. The green vegetation in dry season may be experiencing stress that is reflected in the VGC versus NDVI graph while the vegetation is still green.

The wet season (October – March) and dry season (April – September) correlation curves of NDVI versus total and green VGC are linearly interpolated and applied to the ASTER imagery. This yields total, green and yellow VGC maps and bare soil maps of all (eight) ASTER images. After validation they can be used for spatial and temporal trend analysis. An example of the results is depicted in figure 4.9. Other results can be found in Appendix F.

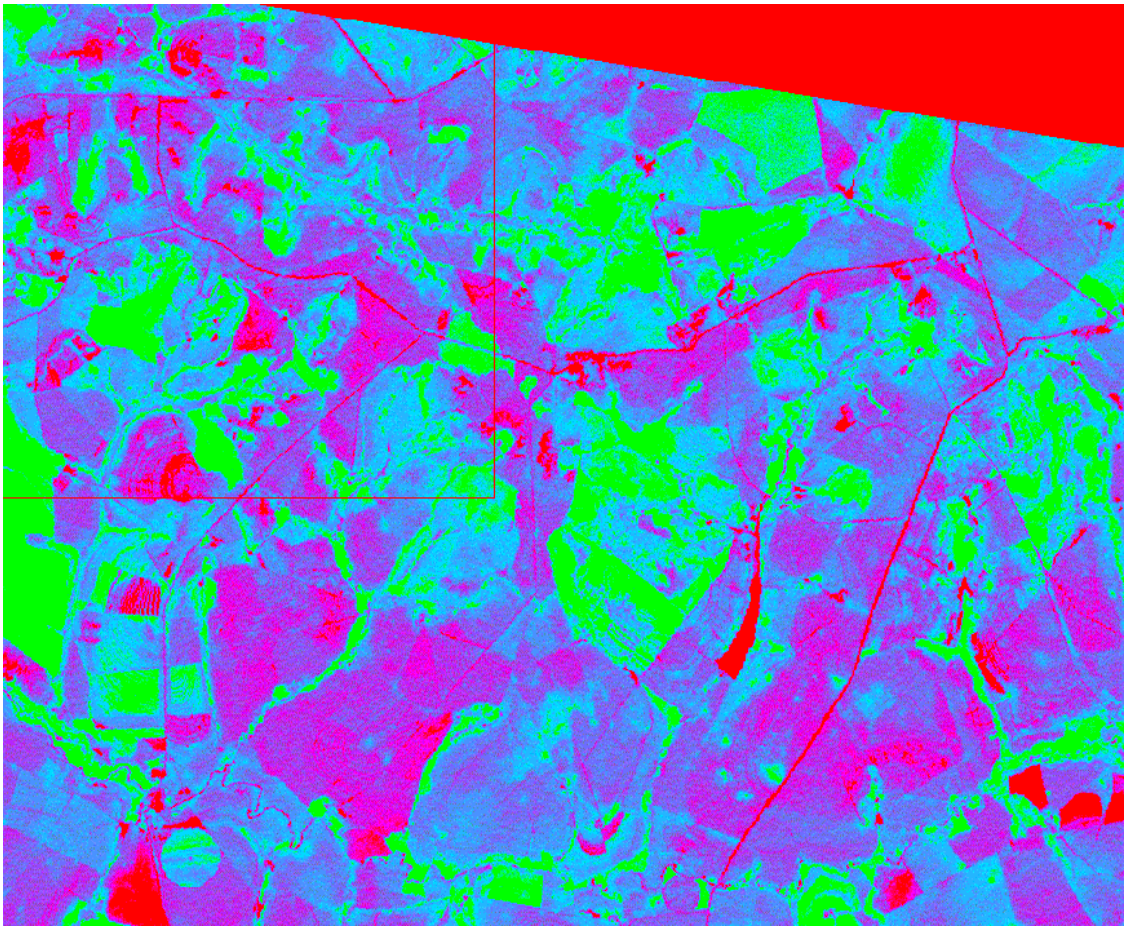

Figure 4.9 Map composition of the VGC maps of level 1B ASTER imagery of 4th March 2003, wet season. (Red: Bare soil, Green. Green vegetation, Blue: Yellow vegetation)

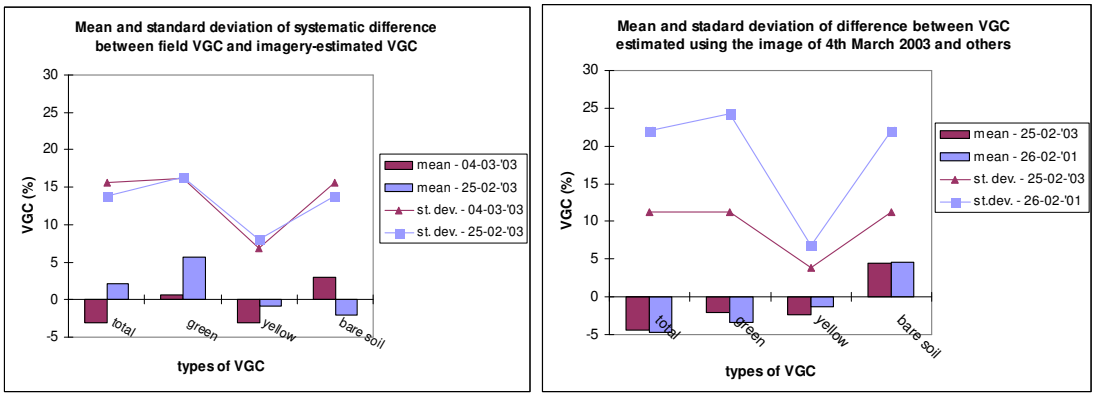

Figure 4.10 Validation results; differences between December 2003 - February 2004 field data (wet season) and level 1B ASTER imagery of 4th March 2003 and of 25th February 2003.

The validation of the results is aiming at on the one hand to get an indication of the accuracy of the VGC-estimate compared to the field data and on the other hand to get an indication of the uncertainty in the VGC-estimate that is caused by using the ASTER image of 4th March 2003 for the derivation of the wet season. The first indication is given by the comparison of the VGC-

imagery estimates and the field VGC estimates. The systematic differences found (figure 4.10a) are 0 to 5 %, the standard deviation belonging to this systematic difference is 5 – 15 %. The mean systematic difference is low, ideally this would be zero, but the variation is high which means that the VGC estimated using the imagery has a high uncertainty. This makes it less suitable for use in erosion models or as a reliable estimate of actual VGC. The low standard deviations found for yellow VGC are caused by the smaller range of yellow VGC occurring in the dataset.

Systematic error caused by using the image of 4th March 2003 to estimate the correlation between wet season field data and wet season ASTER imagery is 0 – 5 % with a standard deviation of 5 – 10 % (figure 4.10b). This is an indication of the height of the actual error by comparing wet season field data of December to (start of) February with imagery from the end of February or beginning of March. Another cause of the systematic difference between the images of February and March 2003 is a difference in viewing angle between the images. This also indicates that the difference of 1 or 2 months between the date of capture of the field data of dry season (July/ August 2002) and the date of the dry season ASTER image (9th September 2002) causes some uncertainty in the results.

An indication of the error made by using wet season field data of 2003/2004 with wet season imagery of (start of) 2003 is derived by comparing the VGC-estimates of the wet seasons of 2001 and 2003 (figure 4.10b).The mean systematic difference in VGC estimates is small, 1-3 %, but the standard deviation is with 5 – 25 % a lot higher than the variation of two images within one year. Part of the standard deviation between the field VGC-estimates and the imagery VGC estimates can therefore probably be explained by the difference of a year between the capture of the field data and the imagery. Another reason for the high standard deviation is that the wet season correlation graphs are derived from 2003 data, while the dry season correlation was derived from 2002 data, creating a gap of one year and different vegetation conditions.

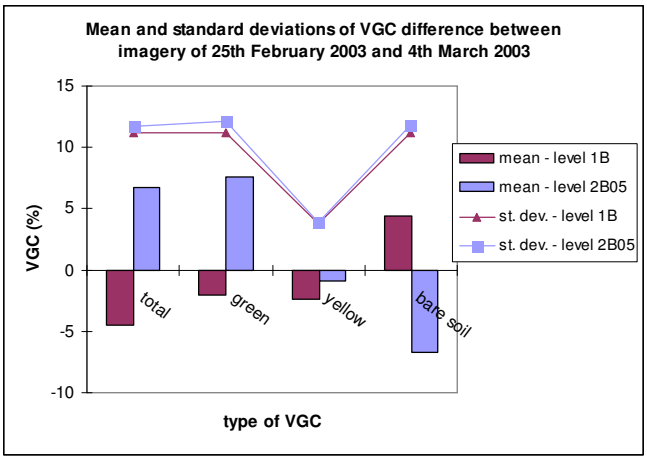

Figure 4.11 Validation results; Differences between the ASTER image of 4th of March 2003 and the 25th of February 2003. Differences are depicted for level 1B (top of the atmosphere radiation) and level 2B05 (surface reflectance) vegetative ground cover maps.

The effect of using level 1B, top of the atmosphere radiance or level 2B05, surface reflectance imagery for the calculation of the VGC maps on the uncertainty of the VGC estimates is tested. The differences between the estimated VGC of 25th February 2003 and 4th March 2003 are calculated for level 1B and level 2B05 imagery. Each level is using their own correlation between 4th March 2003 imagery and wet season field data. The standard deviations are comparable but the order of magnitude of the mean systematic deviation of the level 2B05 imagery is in most cases considerably higher than of the level 1B imagery. Apparently, the correction of solar illumination and atmospheric influences that is performed to derive the level 2B05 is not capable of reducing noise in the level 2B05 data, or the noise in the level 1B data obscured part of the variation present in the reflectance of the area.

Apart from the important factors that are mentioned above general factors that cause the high standard deviations of the systematic difference are in decreasing order of importance:

- Low R^2 values of the correlation curves for dry season and green vegetation. This means a poor correlation and a low accuracy of the VGC estimates.
- The field data of wet season only have 76 green VGC estimations of the 255 total VGC estimations. This means that the correlation between green and yellow VGC with NDVI is less reliable than the correlation of total VGC with NDVI.
- The dry season correlations are estimated using pasture ground truth only, while for wet season field data of all *cerrado* types is used to get a better estimate of the VGC throughout the whole area. This may lead to a possible miss-estimation of the VGC in forest.
- Possible trends in the data due to different (top) soil types. Different soil types have different optical properties that can easily influence the NDVI, especially with a low total VGC.
- The estimation of the VGC in wet season and dry season was performed by different persons, this can lead to standard errors.
- Separation of yellow VGC and litter is spectrally as well as in the field very difficult and may result in errors in the yellow VGC estimation.
- The time difference between the dry season field data and imagery encompasses the first rains of the season, this can lead to errors in the correlation.

4.4 Spatial and temporal dynamics of ground cover

The general temporal trend of the total vegetative ground cover (VGC) is highly dependent on rainfall (figure 4.11 and 4.12). The decrease of green and total VGC starts in April to continue up to September. The increase in yellow vegetation seems to start in April and last until September. In wet season (October – March) total VGC is high and for 50 % green. Total vegetation decreases with 23 % in the course of dry season (April – September) when precipitation declines (figure 2.3). Green VGC is reduced by 25 %, yielding an increase in yellow VGC of 2 %. Standard deviations are high because of variability between and within fields and differences between *cerrado* types (figure 4.13 and 4.14) and the uncertainty in the total VGC estimates described in chapter 4.3. Since the increase in yellow vegetation is only 2 % and the standard

deviation is high, the conclusion must be that it is not possible to accurately detect the yellowing of the VGC in the course of the growing season. The process of decrease of the VGC is better detectable (23 %) and larger than the yellowing of VGC. The 25 % green VGC difference between wet and dry season is compliant with the NDVI green seasonal variations of Ferreira *et al.* (2003) although the relative seasonal variations found by Ferreira differ. Rundquist (2002) finds higher green VGC variations in tallgrass prairie. Total VGC is not comparable due to burning of litter at the prairie at the start of growing season. This indicates that green VGC variations can be higher because obscuring of green VGC by yellow VGC and litter is not possible.

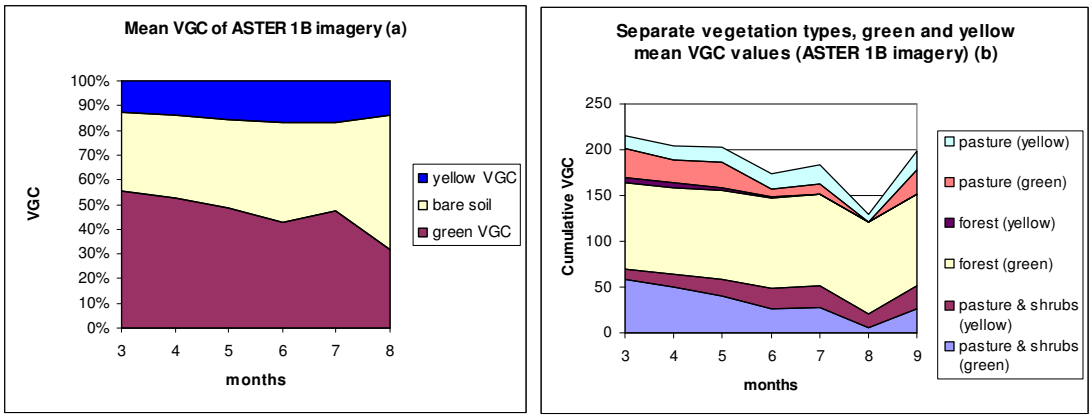

Figure 4.11a, b. a. Mean vegetative ground cover throughout the year (2003) per month of entire research area. (ASTER level 1B imagery). b. Mean VGC of areas of interest selected in forest, pasture & shrubs and pasture. ASTER level 1B imagery.

The total mean VGC is a composite of the different *cerrado* vegetation types; pasture, pasture and shrubs, forest. Analysis of the separate vegetation type results (figure 4.11b), taken at different locations yields the conclusion that total VGC is not influenced by forest, but solely by pasture and pasture and shrubs, of which pasture and shrubs shows the largest VGC variation but has a higher VGC in general. Because the yellow VGC amount is about the same for the two types, the green vegetation makes the difference. The decline of the photo-synthetically active VGC of pasture and shrubs is much larger than the decline of photo-synthetically active VGC pasture (Appendix F). Of pasture and of pasture and shrubs nearly all photo-synthetically active vegetation is green. However, for forest 25 to 40 % of the total vegetation is visibly green but not photo-synthetically active.

To investigate the trend-differences solely caused by radiometric and atmospheric correction of the imagery the NDVI- and VGC-trends of level 1B and level 2B05 ASTER imagery are plotted (figure 4.13a, b, c, d). This also allows for the identification of trend characteristics due to NDVI seasonal differences or to the calculation of the VGC maps.

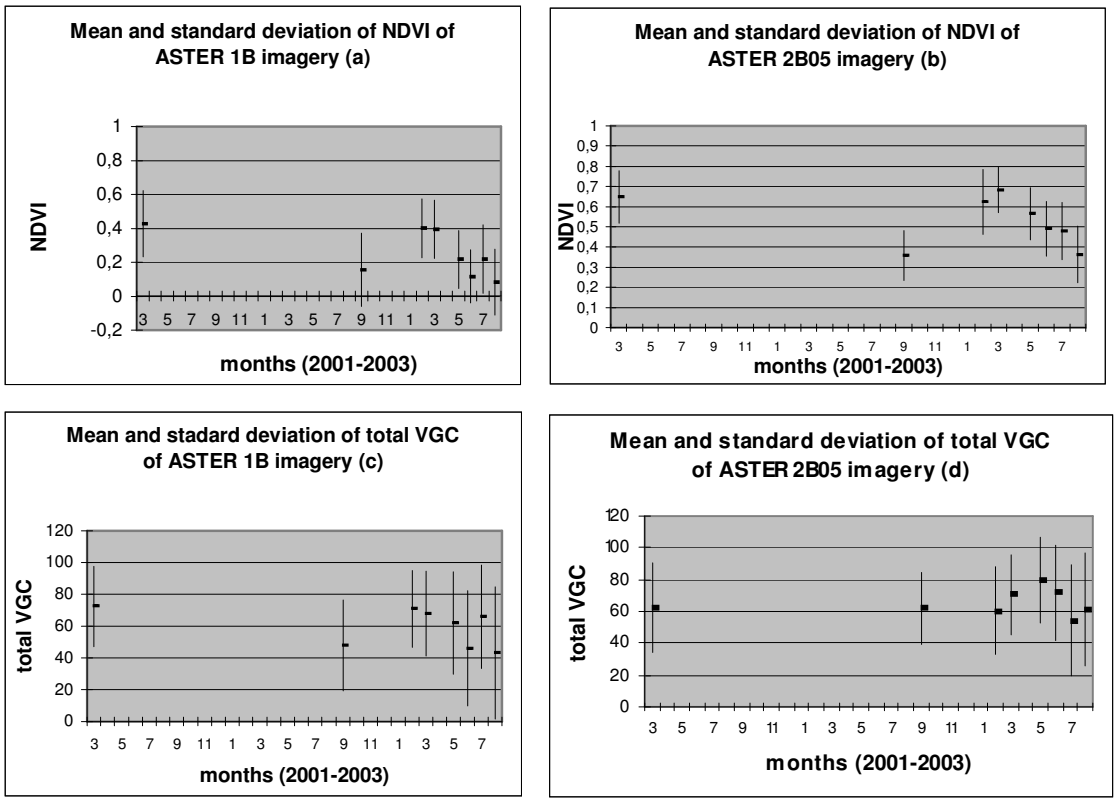

Figure 4.13a, b, c, d. Mean and standard deviation of NDVI (a, b) and total VGC (c, d) of level 1B (a, c) and level 2B05 (b, d) ASTER imagery.

When comparing the VGC trend of ASTER level 1B data and level 2B05 data we conclude that they are much alike. The general trend of a decrease of the VGC in the course of dry season is present and although differences of 10 % VGC occur, the VGC estimates are in the same range. This also holds good for the trends of yellowing and decrease of the vegetation in the course of dry season (Appendix F). The differences between the results for 26th February 2001 and 25th February 2003 are due to the different precipitation amounts in 2001 and 2003. There was less precipitation during the wet season of 2000/2001 as compared to 2002/2003.

Trend-differences between level 1B and level 2B05 VGC maps are a peak in May instead of March of total, especially green, vegetation. Since this difference is not present in the NDVI-trend the probable cause is non-linearity of vegetational change during dry season. The linear interpolation overestimates effects from litter, detectability of seasonal variation etc. as mentioned in chapter 3.3. This peak is not present in level 1B VGC maps because the NDVI difference between 04-03-'03 and 25-02-'03 is much larger, so the overestimation does not alter the trend of declining total VGC at the start of dry season.

The main difference between the NDVI and VGC trends of level 1B and level 2B05 is the high difference in mean value of the image of 24th June 2003 compared to the trend in level 1B data.

This is solved in level 2B05 data. It is therefore due to atmospheric disturbance at 24th June 2003 or an error in the scaling of the digital numbers of the ASTER images.
The NDVI trends resemble the trends found by van Leeuwen and Huete (1996).

After a spatial representation of the VGC maps no clear spatial trends are visible. Neither in the level 1B maps nor in the level 2B05 maps is a gradient present, for example to the river. Trends in the level 1B imagery are the decrease of vegetation especially on the degraded locations with sparse vegetation and the yellowing of the vegetation at places with a high and green VGC. A time-difference is found between the vegetation types. Pasture cover and pasture and shrubs cover starts to decrease in the period between 4th March 2003 and 23rd May 2003 while the forest continues to grow and increase green vegetation after 23rd of May. This produces a rise in vegetation for forest between 4th March 2003 and 11 August 2003 (figure 4.14). Remarkable is that *cerradao*, the original vegetation (top, right of middle figure 4.14) does not show any seasonal change, it is balanced. Overall, total VGC is declining. However, agricultural areas and newly sowed pasture and roads yield a higher VGC in dry season than in wet season.

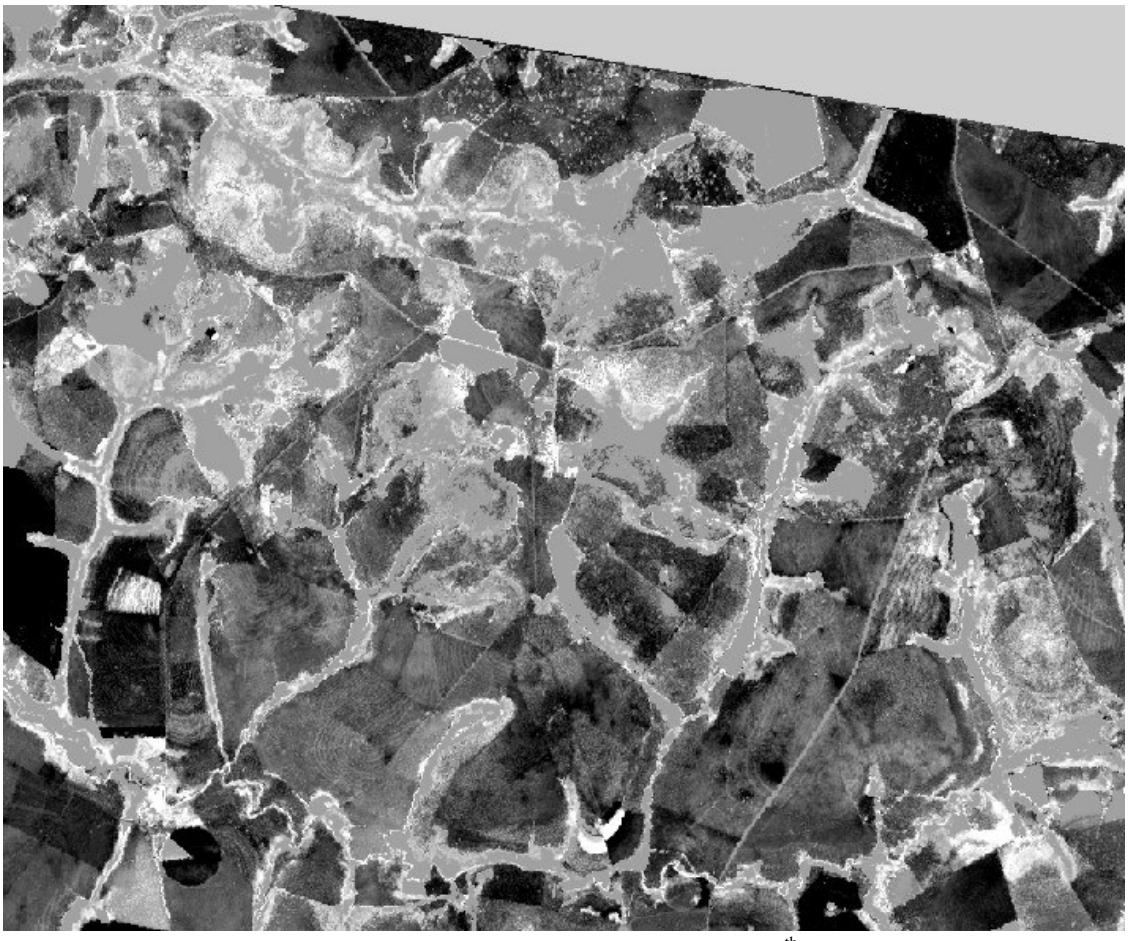

Figure 4.14 Seasonal total vegetation changes. The ASTER 1B image of 4th March 2003 is subtracted from the ASTER 1B image of 11th August 2003. White is an increase of 100% during dry season, black is a decrease of 100%. The large grey areas are zero.

The level 2B05 VGC maps show more or less the same trends as the level 1B VGC maps. The difference is that the forested areas continue to grow until 23rd March 2003. Pasture and shrubs areas are greener during wet season compared to the level 1B VGC maps.

The method is useful for trend estimation and for estimation of the cover percentage, however, there is still a large standard deviation of 10 to 20 percent.

5 General discussion

5.1 Methodology

The objective of this study was to estimate total vegetative ground cover (VGC) using field data and a vegetation index that is used on ASTER imagery. Total VGC comprises both the green and the yellow VGC. The research area is situated near Uberlândia, Central-Brazil. Although the methodology is useful and the estimation of total vegetation cover was reasonably acceptable, the correlation between NDVI and yellow and green vegetation cover is poor. As a consequence, the decrease of vegetation cover in the course of the dry season can be estimated, but the yellowing of the vegetation cannot be detected accurately.

In the majority of studies the (green) vegetative ground cover is based on the NDVI (Normalized Difference Vegetation Index) (equation 3, chapter 3.3.2). Its results thus allow intercomparability of many findings in remote sensing vegetation research. Its application is based on multi-spectral, hyperspectral or field-spectral data. It gives a good estimation of the green vegetative ground cover worldwide and is easy to compute. Drawbacks of the index are its sensitivity to soil brightness and disputed ability to separate yellow or dead-standing non-photosynthetically active biomass or litter from soil (Huete *et al.*, 1985). Although the NDVI has good qualifications for estimating the green vegetative ground cover (VGC), the estimation of total and yellow VGC, both photosynthetically active and non-active vegetation, remains troublesome.

This research shows that the NDVI is capable of making a reasonable estimation of total VGC (R^2 = 0.56, st.dev. = 15) in tropical savannah areas or cerrado if yellow vegetation is included in field estimates of total VGC. This is confirmed by Van Leeuwen and Huete (1996) and Asner (2003). NDVI is known to have difficulties in discriminating sparse green vegetation in a matrix of yellow or non-photosynthetically active vegetation (Numata et al., 2003; Elmore et al., 2000). This is confirmed in this research and underlines the necessity to know the amount of yellow vegetation and litter. Mixed green and yellow vegetation reduce the detectability of both. In order to arrive at a total, green and yellow VGC estimate from NDVI data, the empirical relationships were determined between NDVI and total and green VGC. This yielded an equally poor correlation between green and total VGC versus NDVI in dry season (respectively R^2 = 0.20 and R^2 = 0.16; surface reflectance data) and a poor correlation in wet season of R^2 = 0.19 for green VGC. For total VGC in the wet season a R^2= 0.56 was found for the relation between VGC and NDVI. The explanation of the differences between the $R^2$of total and green VGC in wet season is twofold. A feature of R^2 is that it reacts strongly at points at the outer ends of a linear relationship. If those are not present it will return a low R^2 while the strength of the relationship can be just as strong. The other explanation for the difference in R^2 for wet season is the difficulties encountered in the field to get a good estimate of green vegetation due to the complexity of the area, a very heterogeneous mixture of various species of grass, shrubs, weeds and trees, all with different spectral properties. The higher number of available field data in this category (256 points) underlines the reliability of this relation as compared to the estimated correlation between green VGC and NDVI (76 points).

In general, yellowing of the vegetation causes a drop of the NDVI (Elvidge, 1990; Cyr, 1995; Numata et al., 2003) because the difference between the near-infrared and red bands decreases. This is convenient if the green VGC is needed, but when the total VGC is needed, this decrease in NDVI has to be accounted for to prevent underestimation of total VGC (van Leeuwen and Huete, 1996). In this research, this is tried by calculating the mutual correlation between total, green and yellow VGC with NDVI. A linear relation was found for the correlations between total and green VGC and NDVI (figure 4.7) as did Gao et al.(2000), Rundquist (2002), Zha et al. (2003) and Carlson and Riply (1997). In this way it was possible to distinguish the process of decrease of the VGC. The process of yellowing could not be estimated significantly using the NDVI on ASTER imagery.

Apart from these seasonal trends of decrease and yellowing of the VGC, the NDVI versus VGC relations turned out to be different for wet and dry season. This is due to differences in solar illumination, vegetation composition (Ferreira and Huete, 2003), the relative amount of litter present (van Leeuwen and Huete, 1996), viewing angle differences and scaling of the images. These differences are compensated for by interpolation of the wet season and dry season relations to derive the VGC-maps of all images. These differences are data dependent and for example litter or vegetation composition should be compensated for during data collection and during the procedure of deriving the VGC-maps.

In this research, the seasonal trend of total vegetative ground cover is estimated using wet and dry season field data combined with the NDVI of a series of seven ASTER images throughout a year. This methodology is readily applicable to other research areas. It is especially suitable for diverse land cover systems lacking distinct land cover classes in tropical regions that have a distinct dry season.
Compared to other often applied techniques this methodology offers the following benefits:

- No spectral ground truth is required, just estimations of the VGC that do not need expensive equipment.
- Applicable everywhere in tropical regions where cloud-free ASTER imagery can be acquired for the desired period of the year, although calibration is necessary.
- Designed to be calibrated with mixed and pure pixels, which are present in all imagery.
- Simple procedure without difficult algorithms or models. It works with multi-spectral imagery and is therefore flexible in the choice of sensor, although the precision of the sensor has a direct effect on the precision of the output.
- The NDVI is a widely used index. Results can therefore easily be compared to other research findings.
- The methodology is suitable for trend analysis.

Drawbacks of this methodology are the high amount of ground truth that is required both in wet and in dry season to get a good estimation of the VGC - NDVI correlation. Furthermore, the uncertainty of VGC estimates is high. Although the systematic error is only 0-5 %, the standard deviation of the systematic error of 10-20 % compared to the field data is high. This has a number

of reasons that are described in chapter 4.3, which can be reduced but not eliminated. The NDVI is sensitive to soil brightness. If the method is applied elsewhere this should be taken into account. Soil brightness was not compensated for in this research because the area has a more or less homogeneous soil type and soil background. Another possible source of error is the difficulty of distinguishing litter spectrally or in the field from yellow VGC. Although both important the litter and the yellow VGC have a different influence on the impact of precipitation on erosion. This should be resolved during the calibration, but a bias in the field data is likely since the two are often difficult to separate. Finally, errors in radiometric or geometric correction of the imagery have a direct effect on the quality of the results.

5.2 Annual trends

Erosion is a world-wide acknowledged threat to sustainable agriculture and is mainly caused by disruption of the natural equilibrium of an ecosystem (Laflen and Roose, 1997). This man-made disruption of the vegetation equilibrium is once again proved by the results of this research. The locations that still inhabit *cerradao,* an original dense *cerrado* formation, or Gallery forest show no to little change in total, green or yellow vegetative ground cover (VGC) in the transition from wet to (the end of) dry season. This is in sharp contrast to the man-made agricultural land cover of that replaces the original *cerrado* vegetation and mainly consists of pastures, sometimes with shrubs and of some crops.

This research aims at estimation of the total vegetative ground cover all year round. Since yellow vegetation is still able to protect the soil against erosion, this plays a crucial role while a VGC below 70 % already causes a high erosion risk (Cyr *et al.*, 1995). Although the approach used is useful, in this study it was not successful in estimating yellow VGC or in detecting the process of yellowing of the vegetation. Forests have a constant cover of 100% but start to decrease photosynthetic activity in May while the pastures start degrading and yellowing between March and May. This is due to the deeper rooting depth of trees allowing a prolonged use of soil moisture compared to pasture. The non-forested area is most sensitive to erosion from August until October because then the total VGC is at a minimum and heavy precipitation starts. After October probably part of the vegetation has regrown. The general trend and the differences in NDVI (Normalized Difference Vegetation Index) response of the different vegetation types are coherent with Ferreira *et al.* (2003). The vegetation dynamics are primarily influenced by precipitation although management guarding the quality of the pasture cover, like preventing overgrazing and resowing, is able to limit degradation due to a low VGC to a certain extent.

5.3 Suggestions to improve the estimation of the total vegetative ground cover

In most cases when yellow vegetation has to be estimated, (linear) spectral unmixing is applied (Asner and Heidebrecht, 2002; Elmore *et al.*, 2000; Roberts *et al.*, 1997). Spectral unmixing (SMA) is based on the assumption that the spectrum measured by a sensor is a linear or nonlinear combination of the spectra of components within the instantaneous field of view (IFOV) (Roberts

et al., 1997). This technique is capable of making a robust estimate of vegetative ground cover (VGC) change and estimation of VGC amounts (Elmore, 2000). In *cerrado* vegetation as in other very heterogeneous ecosystems spectral unmixing can lead to erroneous results because of difficulties in selecting pure endmember spectra that are vital to a good result. Compared to spectral unmixing this study requires more field data to allow a reliable estimation of VGC, while the number of field data needed increases with the complexity of the vegetation as this approach needs calibration to each study area and vegetation type where it is applied. Further research is desirable to minimize both the number of field data in different field situations and influences on the quality of the VGC estimations.

Although the approach used in this study yielded results comparable to Asner *et al.* (1999), the quantification of yellow or non-photosynthetically active vegetation can be improved. In general, NDVI is assumed to have major drawbacks and is mainly focussed on green vegetation (Asner *et al.*, 1999; Carlson and Riply, 1997) but in combination with spectral data in the short wave infrared (SWIR) a good estimation of non-photosynthetically active vegetation is possible (Asner *et al.*, 1999; Numata *et al.*, 2003; Asner *et al.*, 2000). Asner *et al.* (1999) describes absorption features associated with bare soil at 2200 nm and with non-photosynthetically active vegetation at 2000 and 2075 nm. The absorption features of lignin and cellulose, the plant material that enables the discrimination of bare soil and vegetation, are centred near 1730, 2060 and 2270 nm (Roberts *et al.*, 1997). Some research is done by Asner and Heidebrecht (2002) using these features in the SWIR in a spectral unmixing procedure to separate bare soil and photosynthetically active and non-active vegetation. The possibilities of using the SWIR-range in a comparable way as the red, near-infrared range in this research should be further explored using ASTER imagery. A normalized difference vegetation index using ASTER band 6 (2.185-2.225 nm) and 7 (2.235-2.285 nm) might allow a better distinction between vegetative ground cover and bare soil. ASTER bands 5 to 9 (2.145-2.365 nm) were not used in this current research because the spectral differences between the green and yellow VGC and bare soil are small (figure 4.1). The possibilities should be further explored with the wet season data and more training sites. Still, figure 4.1 indicates that a distinction between vegetation and bare soil is possible in the SWIR. This could be combined with the use of NDVI in the red and near-infrared to discriminate between healthy and yellow vegetation or dead standing biomass.

Compared to other multi-spectral sensors ASTER has a lot of bands in the SWIR. The red and near-infrared ASTER bands (band 2 and 3) are relatively narrow and able to show both sides of the red edge position without the chance that part of the actual edge itself is captured. The performance of ASTER (with the spatial resolution of 15 m) was therefore satisfactory. In the current heterogeneous area a finer resolution would probably reduce errors in the estimation of the VGC because separate bushes or features smaller than 7 m cannot be detected.

Another option to enhance the results while still using a combination of NDVI and field data is to use hyperspectral imagery. Because the bandwidths are much smaller, 1 or 2 nm, the absorption features of lignin and cellulose can probably be detected, thus retrieving a more robust estimate of the yellow VGC. However, although there is a large number of mostly airborne hyperspectral

sensors, the multi-spectral imagery is more widely used and mostly spaceborne. They are therefore regularly available all around the world, which enables applications at a larger extent.

An option to improve the linear relation between the vegetative ground cover and NDVI is to further adjust the collection of field data to the research purpose at hand. While keeping the advantage of estimating vegetative ground cover in the field without the use of a spectrometer, improvements of the method of field sampling can be:

- Estimation of total, green and yellow vegetative ground cover of all locations.
- Sample the same locations in a subsequent wet and dry season.
- Select locations for sampling of about 30 m^2 with a more or less homogeneous cover.
- Collect samples of the minimum and maximum (total) vegetative ground cover on each field or *cerrado* formation.

Another big improvement of the results of this study can be achieved by collecting field spectra of the main species in their main phenological stages, green, yellow and litter phase. Using this data can help discriminating between the green, yellow and litter VGC and may improve stratification results if the vegetative ground cover field estimations are also taken of different species or *cerrado* types.

Nog uitwerken in een kort stukje:

- Are other indices more suitable for this research? SAVI or a combination of indices, perhaps combined with spatial statistics can yield an improvement.

6. Conclusions

Main conclusions of this research are:

- The yearly development of total vegetative ground cover (*cerrado* vegetation) in a research area near Uberlândia, Central Brazil could be estimated with a standard deviation of 15 % vegetative ground cover from field data of two seasons and a series of Normalized Difference Vegetation Indices (NDVI) derived from ASTER imagery. The separate yellow and green estimates of vegetative ground cover (VGC) from NDVI are poor ($R^2 = 0.2$) and give merely an indication of the spatial distribution of VGC differences.
- The NDVI, based on the red and infrared wavelengths, is reasonably correlated with field data of total VGC ($R^2 = 0.55$).
- Stratification to vegetation types does not yield an overall better estimation of the VGC.
- Especially in dry season the presence of yellow vegetation weakens the NDVI versus VGC relation. To prevent underestimation of total vegetative ground cover yellow vegetative ground cover thus should be included in the estimation of total VGC.
- Of the two vegetational trends in the area, the decrease of VGC in the course of the dry season can be estimated but the yellowing of the vegetation cannot be estimated significantly using satellite imagery.
- A large difference was found between the relation of total vegetative ground cover with NDVI for wet and for dry season. To get a good estimate of the total vegetative ground cover, field data in wet (October – March) and dry season (April – September) should be available. The relation was interpolated for the images between wet and dry season.
- The estimation of the total vegetative ground cover of the surface reflectance imagery and the top-of-the-atmosphere imagery performed more or less similar. The systematic mean deviations between the estimated and the field total vegetative ground cover are higher for the surface reflectance imagery than for the top-of-the-atmosphere imagery although the surface reflectance imagery is expected to perform better because differences in solar illumination, solar angle, scaling and atmospheric distortion are corrected for.

- The different *cerrado* formation types (forest, pasture and shrubs, pasture) have clear differences in their annual vegetative ground cover dynamics. The original *cerradao* vegetation does not show seasonal vegetation dynamics. Pasture is most sensitive to erosion although the seasonal dynamics of pasture and shrubs are larger, both starting to decrease VGC in March, April. Forests start to reduce photosynthetic activity in May and have no variations in total vegetative ground cover.
- The area and especially the part covered with pasture are most sensitive to erosion from August to October, because of a low VGC and wet season starting in September.

7. Recommendations

Recommendations for further research are:

- Validation of the dry season estimates of the vegetative ground cover (VGC).
- Testing the quality of the results if only pasture vegetative ground cover is estimated. In this study all *cerrado* types are estimated, using the derived linear relation between total vegetative ground cover and NDVI for wet season. For the dry season the relation between only pasture total vegetative ground cover and NDVI was used.
- Other possible methods to interpolate the relations between total vegetative ground cover and NDVI can be tested, e.g. scaling the relation to the minimum and maximum NDVI found in an image to eliminate scaling differences of the radiometric correction.
- Other vegetation indices like SAVI can be tested on their performance and error ranges in the *cerrado* environment.
- Literature indicated that the short wave infrared (SWIR) has good potential for discriminating yellow and green vegetation and bare soil. A drawback is the 30 m resolution of ASTER in the SWIR and the relatively large bandwidths. Research in the use of SWIR for discriminating yellow vegetation, in combination with NDVI is promising.
- Improve the collection of field data.
- Measurement of field-spectra of the various vegetation and soil types at different phenological stages with a (hyper)field spectrometer to enable a better link between vegetative ground cover of different vegetation types and covers with as estimated from remote sensing satellite imagery.
- The use of hyperspectral imagery is promising because smaller changes in spectral behaviour of the vegetation can be traced, which can lead to a better discrimination between yellow vegetation and bare soil, also in the red and near-infrared wavelengths.
- Estimation of the total vegetative ground cover and regrowth of the vegetation in September to November with field data and ASTER imagery of that period. This is the period when the area is most sensitive to erosion.
- Combination of the trend-results of this study with actual erosion rate data in wet and dry season.
- Modelling the vegetative ground cover dynamics as a function of precipitation.

Literature

Asner, G. P., M.M.C. Bustamante, A.R. Townsend, (2003), Scale dependence of biophysical structure in deforested areas bordering the Tapajos National Forest, Central Amazon, *Remote Sensing of Environment* 87 4: 507-520

Asner, G.P., K.B. Heidebrecht, (2002), Spectral unmixing of vegetation, soil and dry carbon cover in arid regions: comparing multispectral and hyperspectral observations, *International Journal of Remote Sensing* 23, 19: 3939-3958

Asner, G.P., A.R. Townsend, M.M.C. Bustamante, (1999), Spectrometry of pasture condition and biogeochemistry in the Central Amazon, *Geophysical Research Letters* 26 17: 2769-2772

Asner, C.A. Wessman, C.A. Bateson, J.L. Privette, (2000), Impact of tissue, canopy, and landscape factors on the hyperspectral reflectance variability of arid ecosystems, *Remote Sensing of Environment* 74: 69-84

Baccaro, C.A.D., (1999), Processos Erosivos no Domínio do Cerrado, Capítulo 6, In A.J. Guerra *et al.* and B. Brasil (editor), Erosão e Conservação dos Solos

Baret, F., G. Guyot, (1991), Potentials and limits of vegetation indices for LAI and APAR assessment, *Remote Sensing of Environment* 35 2-3: 161-173

Bennett, H.H., (1939) Soil Conservation, McGraw-Hill, New York, NY USA

Biard, F., F. Baret, (1997), Crop Residue Estimation Using Multiband Reflectance, *Remote Sensing of Environment* 59 3: 530-536

Bonn, F., J. Mégier, A. Ait Fora, (1997), Remote sensing assisted spatialization of erosion models within a GIS for land degradation quantification: Expectations, errors and beyond…, *Remote Sensing '96, Spiteri (ed.)*: 191-198

Borel, C.C., S.A.W. Gerstl, (1994), Non-linear spectral unmixing models for vegetative and soil surfaces, *Remote Sensing of Environment* 47 3: 403-416

Carlson, T.N., D.A. Riply, (1997), On the relation between NDVI, Fractional Vegetation Cover, and Leaf Area Index, *Remote Sensing of Environment* 62 3: 241-252

Carreiras, J.M.B., Y.E. Shimabukuro, J.M.C. Pereira, (2002), Cover fraction images derived from SPOT-4 Vegetation data to assess land-cover change over the State of Mato Grosso, Brazil, *International Journal of Remote Sensing* 23 23: 4979-4983

Cyr, L., F. Bonn, A. Pesant, (1995), Vegetation indices derived from remote sensing for an estimation of soil protection against water erosion, *Ecological Modelling* 79: 277-285

Department of Natural Resources and Environment (DNRE), (2004), Landcare Field Guide, http://www.netc.net.au/enviro/fguide/gullero.html

Driessen, P.M., R. Dudal, (1991), Major Soils of the World, Wageningen Agricultural University, Katholieke Universiteit Leuven

Elmore, A.J., J.F. Mustard, S.J. Manning, D.B. Lobell, (2000), Quantifying vegetation change in semi arid environments: Precision and accuracy of spectral mixture analysis and the Normalized Difference Vegetation Index, *Remote Sensing of Environment* 73 1: 87-102

Elvidge, C.D., (1990), Visible and near-infrared reflectance characteristics of dry plant materials, *International Journal of Remote Sensing* 11 10: 1775-1795

EMBRAPA, (1982), Serviço Nacional de Levantamento, Conservação de Solos – EMBRAPA, Levantamento de Reconhecimento de Média Intensidade dos Solos e Avaliação da Aptidao Agrícola das Terras do Triãngulo Mineiro, *Boletim de Pesquisa* no. 1, Rio de Janeiro

FAO, (2001), Major Soils of the World, *World Soil Resources Reports* 94

Ferreira, L.G., A.R. Huete, (2004), Assessing the seasonal dynamics of eth Brazilian Cerrado vegetation through the use of spectral vegetation indices, *International Journal of Remote Sensing* 25 10:1837-1860

Ferreira, L.G., H. Yoshioka, A. Huete, E.E. Sano, (2003), Seasonal landscape and spectral vegetation index dynamics in the Brazilian Cerrado: An analysis within the Large-Scale Biosphere_Atmosphere Experiment in Amazônia (LBA), *Remote Sensing of Environment* 87:534-550

Galvão, L.S., F.J. Ponzoni, J.C.N. Epiphanio, B.F.Y. Rudorff, A.R. Formaggio, (2004), Sun and viewing angle effects on NDVI determination of land cover types in the Brazilian Amazon region with hyperspectral data, *International Journal of Remote Sensing* 25 10:1861-1879

Gao,X., Huete, A.R., W. Ni, T. Miura, (2000), Optical-biophysical relationships of vegetation spectra without background contamination, *Remote Sensing of Environment* 74 3: 609-620

Hashem, N., N.A. Drake, J. Wainwright, (2000), High Spatial Resolution Remote Sensing for Soil Erosion Modelling

Hernández Morcillo, M., (2004), Analysis of gully retreat in the Brazilian Cerrados using aerial photography and QuickBird imagery, *MSc thesis report Wageningen University*

Hostert, P., A. Roder, J. Hill, (2003), Coupling spectral unmixing and trend analysis for monitoring of long-term vegetation dynamics in Mediterranean rangelands. *Remote Sensing of Environment* 87 2-3: 183-197

Huete, A.R., (1988), A soil-adjusted vegetation index (SAVI), *Remote Sensing of Environment* 25 3:295-309

Huete, A.R., R.D. Jackson, D.F. Post, (1985), Spectral response of a plant canopy with different soil backgrounds, *Remote Sensing of Environment* 17: 37-53

Idso, S.B., P.J. Pinter Jr., R.D. Jackson, R.J. Reginato, (1980), Estimation of grain yields by remote sensing of crop senescence rates, *Remote Sensing of Environment* 9 1: 87-91 *Short Communication*

Ishiyama, T., Y. Nakajima, Koji Kajiwara, K. Tsuchiya, (1997), Extraction of vegetation cover in an arid area based on satellite data, *Advanced Space Research* 19 no. 9: 1375-1378

Jong, de, S.M., (2004), Volcano kills trees by toxic gasses,
http://www.frw.ruu.nl/fg/volcanoes.html, University of Utrecht

Kilewe, A.M., and L.G. Ulsaker, (1984), Soil erosion: A Threat to Land Resources, *East African Agricultural and Forestry Journal, Special Issue* 44: 203-209

Laflen, J.M., E.J. Roose, (1997), Methodologies for Assessment of Soil Degradation Due to Water Erosion. In: R. Lal, W.H. Blum, C. Valentine, and B.A. Stewart (Editors), Methods for Assessment of Soil Degradation. CRC Press LLC, USA

Lal, R., (1990), Soil Erosion in the Tropics: Principles and Management. McGraw-Hill Inc., USA

Leeuwen, van, W.J.D., A.R. Huete, (1996), Effects of standing litter on the biophysical interpretation of plant canopies with spectral indices, *Remote Sensing of Environment* 55:123-138

Lillesand, T.M., R.W. Kiefer, (2000), Remote Sensing and Image Interpretation, 4th edition, John Wiley & Sons Inc.

Maldonado, F.D., J.R. Dos Santos, V.C. De Carvalho, (2002), Land use dynamics in the semi-arid region of Brazil (Quixaba, PE): characterization by principal component analysis (PCA), *International Journal of Remote Sensing* 23-23: 5005-5013

Neufeldt, H., M. de Oliviera Schneider, W. Zech, Oxisol Development along a compound catena of the Araguari river, Central Brazil. In: Thomas, R. and Ayarza, M.A., (1999), Sustainable land

management for the Oxisols of the Latin American savannas. Centro Internacional de Agricultura Tropical. Cali, Colombia.

Nill, D., U. Schwertmann, U. Sabel-Koschella, M. Berhard, J. Breuer, (1996), Soil Erosion by water in Africa: Principles, Prediction and Protection, Deutsche Gesellschaft für Technische Zusammenarbeit (GTZ) GmbH

Numata, I., J.V. Soares, D.A. Roberts, F.C. Leonidas, O.A. Chadwick, G.T. Batista, (2003), Relationships among soil fertility dynamics and remotely sensed measures across pasture chronosequences in Rondonia, Brazil, *Remote Sensing of Environment* 87 4: 446-455

Okoth, P.F., (2003), A Hierarchical Method for Soil erosion Assessment and Spatial Risk Modelling: A Case Study of Kiambu District in Kenya, *PhD-thesis Wageningen University*

Price, K.P., X. Gao, J.M. Stiles, (2002), Comparison of Landsat TM and ERS-2 SAR data for discriminating among grassland types and treatments in eastern Kansas, *Computers and Electronics in Agriculture* 37 1-3: 157-171

Roberts, D.A., M.O. Smith, J.B. Adams, (1993) Green vegetation, nonphotosynthetic vegetation, and soils in AVIRIS data, *Remote Sensing of Environment* 44: 255-269

Roberts, D.A., R.O. Green, J.B. Adams, (1997), Temporal and spatial patterns in vegetation and atmosphere properties in AVIRIS, *Remote Sensing of Environment* 62: 223-240

Rundquist, B.C., (2002), The influence of green vegetation fraction on spectral measurements over native tallgrass prairie, *Remote Sensing of Environment* 81: 129-135

Schok, H.A., J.G.P.W. Clevers, (2001) Remote Sensing 2 Exercises, practical manual for K075-218/K075-209 06192303 Wageningen University

Seyler, F., V. Chaplot, F. Muller, C.E.P. Cerri, M. Bernoux, V. Ballester, C. Feller, C.C.C. Cerri, (2002), Pasture mapping by classification of Landsat TM images. Analysis of the spectral behaviour of the pasture class in a real medium-scale environment: the case of the Piracicaba Catchment (12 400 km^2, Brazil), *International Journal of Remote Sensing* 23-23: 4985-5004

Thomas, R. and Ayarza, M.A., (1999), Sustainable land management for the Oxisols of the Latin American savannas. Centro Internacional de Agricultura Tropical. Cali, Colombia.

Tucker, C.J., (1977) Spectral estimation of grass canopy variables, *Remote Sensing of Environment* 6 1: 11-26

Vrieling, A., (2003), Regional erosion risk mapping in tropical environments using multi-temporal satellite data, http://www.dow.wau.nl/eswc/phd_anton.htm#introduction

Wooley, J.T., (1971), Reflectance and Transmittance of Light by Leaves, *Plant Physiology* 47: 656-662

Zha, Y., J. Gao, S. Ni, Y. Liu, J. Jiang, Y. Wei, (2003), A spectral reflectance-based approach to quantification of grassland cover from Landsat TM imagery, *Remote Sensing of Environment* 87 2-3: 371-375

Appendices

Appendix A: Darkest Pixel Analysis parameters

	26-02-'01	09-09-'02	25-02-'03	04-03-'03	23-05-'03	17-06-'03	24-06-'03	11-08-'03
band 1	27	48	39	42	18	31	32	37
band 2	17	29	17	13	10	7	15	19
band 3	19	16	21	21	14	11	12	14
band 4	19	22	9	15	13	7	12	17
band 5	15	14	12	11	1	9	9	1
band 6	1	1	1	9	1	1	6	1
band 7	17	1	9	1	1	1	8	1
band 8	1	1	8	8	1	1	1	1
band 9	4	1	1	1	1	2	1	3

Digital numbers that are subtracted from the original bands of the ASTER imagery per date. (Chapter 3.2 and 4.1)

Appendix B: Geometrical correction parameters

11-08-'03 ASTER using a Landsat image

control point error (Landsat pixelsize):

x	0,9567
y	0,8835
total	1,3022

1st order polynomial model:

	x'	y'
constant	-70192,3	134156,0
x	0,0658	0,0109
y	-0,0109	0,0658

26-02-'01 ASTER to 11-08-'03 ASTER

control point error (ASTER pixelsize):

x	0,3091
y	0,3209
total	0,4456

1st order polynomial model:

	x'	y'
constant	39396,6	-523418
x	0,0658	0,0109
y	-0,0109	0,0658

09-09-'02 ASTER to 11-08-'03 ASTER

control point error (ASTER pixelsize):

x	0,3916
y	0,3070
total	0,4976

1st order polynomial model:

	x'	y'
constant	40019,5	-523493
x	0,0658	0,0109
y	-0,0109	0,0658

04-03-'03 ASTER to 11-08-'03 ASTER

control point error (ASTER pixelsize):

x	0,3589
y	0,3962
total	0,5345

1st order polynomial model:

	x'	y'
constant	39186,5	-523498
x	0,0658	0,0109
y	-0,0109	0,0658

23-05-'03 ASTER to 11-08-'03 ASTER

control point error (ASTER pixelsize):

x	0,3031
y	0,3250
total	0,4445

1st order polynomial model:

	x'	y'
constant	37380	-523543
x	0,0659	0,0109
y	-0,0109	0,0658

17-06-'03 ASTER to 11-08-'03 ASTER

control point error (ASTER pixelsize):

x	0,3379
y	0,3766
total	0,5060

1st order polynomial model:

	x'	y'
constant	41269,3	-524815
x	0,0657	0,0115
y	-0,0115	0,0657

24-06-'03 ASTER to 11-08-'03 ASTER

control point error (ASTER pixelsize):

x	0,2784
y	0,3434
total	0,4421

1st order polynomial model:

	x'	y'
constant	39768,3	-523495
x	0,0658	0,0109
y	-0,0109	0,0658

Appendix C: Spectral signature graphs

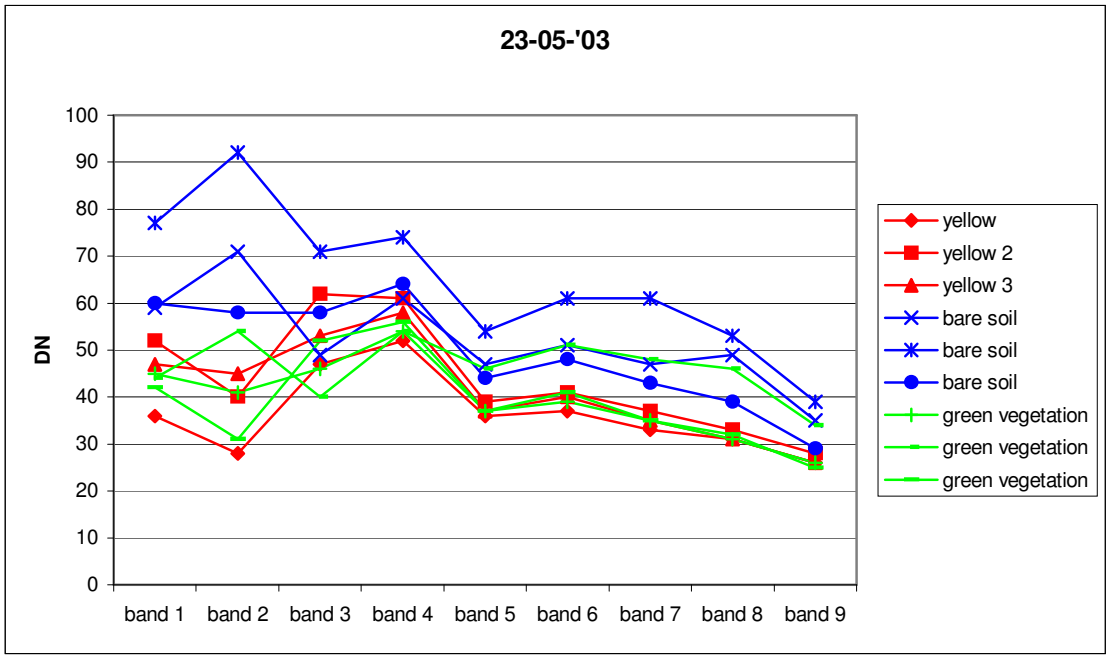

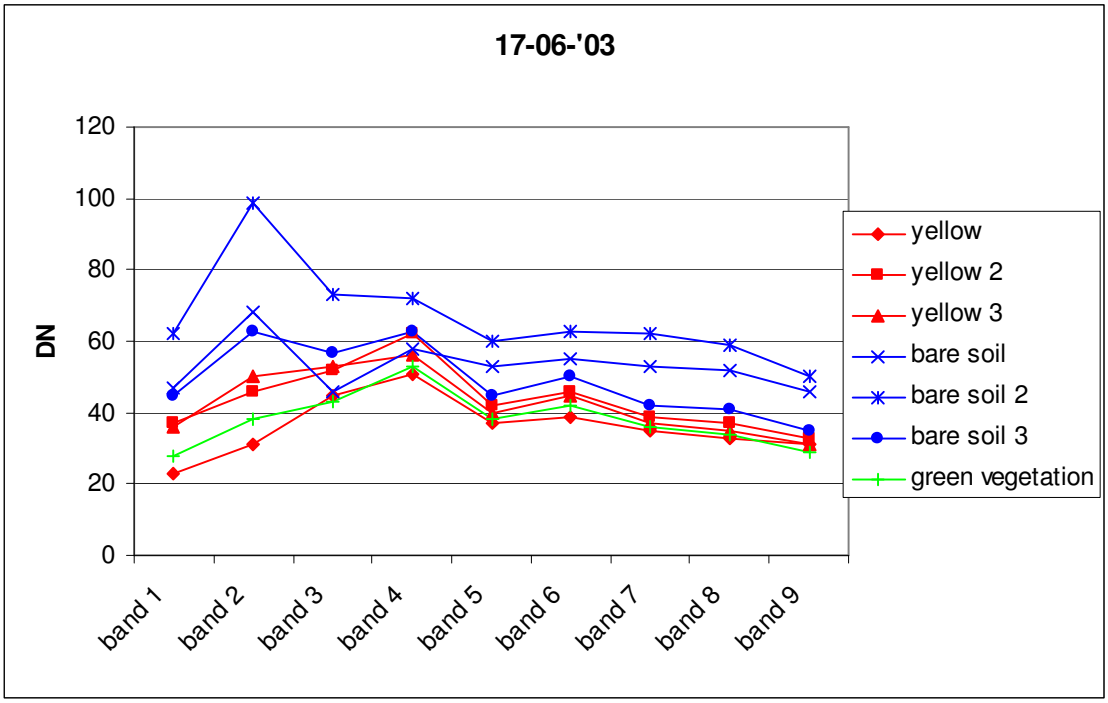

Two spectral signatures of yellow and green vegetation and bare soil of ASTER level 1B (top of the atmosphere radiance). The classification of the signatures is derived from ground truth of August 2002. The dates of the imagery are the 23rd of May 2003 (upper) and the 17th of June 2003 (lower).

Appendix D: Spectral scatter plots

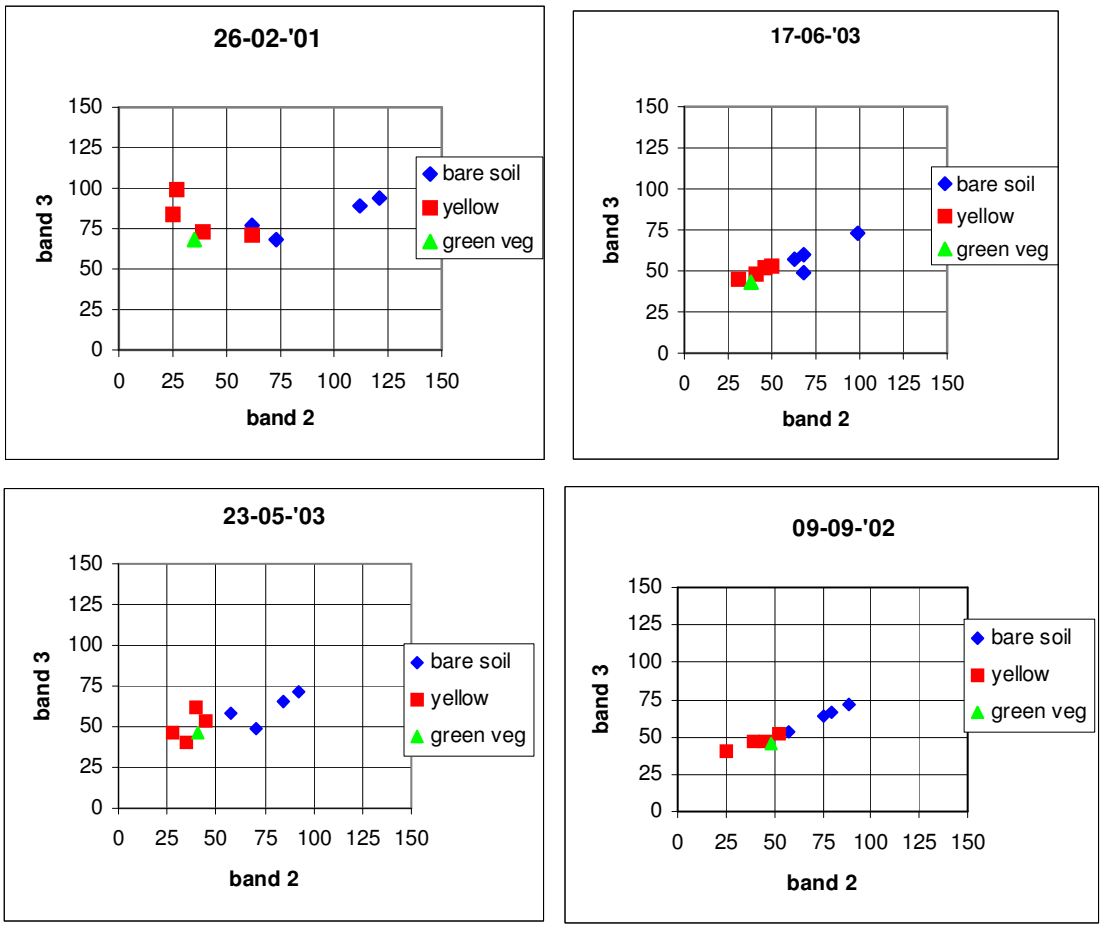

Scatterplots of band 2 (red) and band 3 (near-infrared) of ASTER level 1B imagery (top of the atmosphere radiance). Locations are chosen using groundtruth of August 2002.

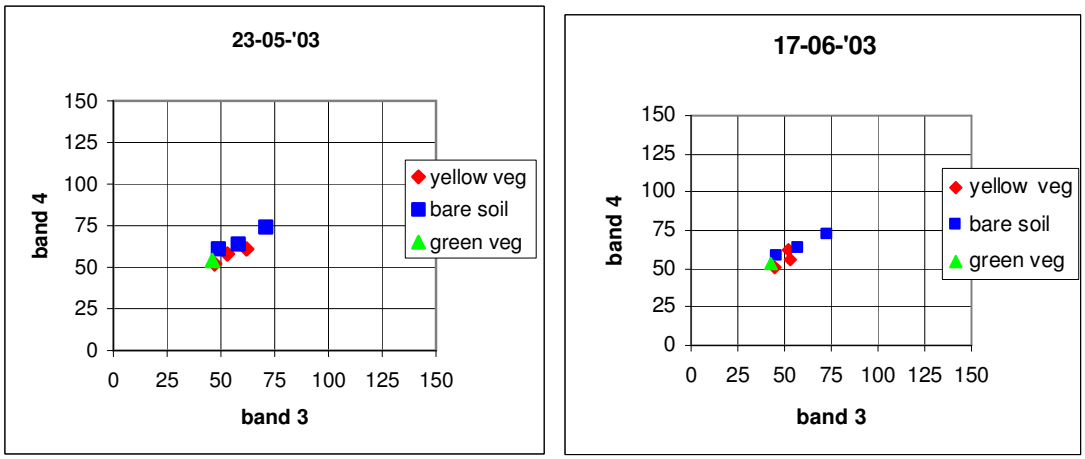

Scatterplots of band 3 (near-infrared) and band 4 (short wave infrared) of ASTER level 1B imagery (top of the atmosphere radiance). Locations are chosen using groundtruth of August 2002.

Appendix E: Dry season vegetative ground cover field estimates

Filename	Geographic coordinates		estimated field VGC		UTM-SAD 69 coordinates		NDVI of 09-09-'02 ASTER
	y	x	green	total	x	y	
groundcover-pasture_N	19 01 06	48 29 27.2	5	80	764122,5	7895251,6	0,055
groundcover	19 01 17.4	48 24 51	10	70	772197,0	7894785,1	0,083
groundcover	19 01 23.5	48 25 32.9	5	90	770969,6	7894613,2	0,077
groundcover_W	19 01 25.6	48 23 58.8	0	90	773720,8	7894508,9	-0,018
groundcover	19 01 29.8	48 24 41.1	0	95	772478,7	7894391,8	0,135
pasto_cover	19 01 43.2	48 24 00.3	5	95	773669,6	7893967,4	0,020
cover_grassland	19 01 50.5	48 24 28.7	5	90	772835,4	7893755,2	0,019
groundcover_S	19 01 52	48 24 55.6	5	100	772047,0	7893720,5	0,021
groundcover_S	19 02 23.4	48 26 10	5	80	769857,3	7892787,5	0,135
pasture-groundcover	19 02 23.4	48 27 49.3	30	90	766950,6	7892829,6	0,011
groundcover_N	19 02 28	48 27 02.6	5	70	768315,2	7892668,6	0,000
groundcover_SE	19 02 28	48 27 02.6	10	65	768315,2	7892668,6	0,000
groundcover	19 02 39.5	48 27 15.6	30	60	767931,1	7892321,0	0,021
groundcover_S	19 02 46.6	48 28 12.3	15	60	766268,3	7892125,3	0,043
pasture_groundcover	19 02 51.5	48 25 35.7	60	100	770847,0	7891907,6	0,087
pasture_groundcover	19 03 05.5	48 27 18.9	30	100	767823,2	7891519,8	0,067
groundcover	19 03 10.3	48 26 51.5	10	80	768622,6	7891362,5	0,030
pasture_groundcover	19 03 12	48 27 20.8	35	100	767764,6	7891322,3	0,114
pasture_groundcover	19 03 16.6	48 26 52.2	5	90	768598,8	7891168,6	0,011
groundcover_pasture	19 03 20.3	48 28 48.2	5	90	765203,6	7891102,8	0,077
pasture_groundcover	19 03 20.7	48 27 03.7	20	100	768260,4	7891046,0	0,130
groundcover	19 03 28.9	48 24 20	0	60	773045,8	7890725,9	-0,020
groundcover+pasture	19 03 49.9	48 29 16.6	0	90	764362,1	7890204,6	0,011
pasture_groundcover	19 04 11.6	48 29 30.8	5	100	763935,9	7889544,2	0,032
groundcover_SE	19 04 49.7	48 29 26.1	0	90	764054,8	7888369,8	0,068
pasture-groundcover_NE	19 04 49.7	48 29 26.1	20	90	764054,8	7888369,8	0,111
pasture-groundcover_SW	19 04 49.7	48 29 26.1	35	80	764054,8	7888369,8	0,023
groundcover	19 05 10.4	48 25 07.1	10	70	771620,8	7887623,4	0,000
grama_cover	19 05 54.4	48 25 58.8	50	80	770089,7	7886291,7	0,046
groundcover	19 05 55.3	48 25 29.4	10	60	770949,4	7886240,5	0,075

Examples of the estimation of the total and green vegetative ground cover as depicted in the table above are given by the following (nadir) ground cover pictures together with the estimated total and green vegetative ground cover (VGC).

Filename	Geographic coordinates y	x	estimated field VGC green	total	UTM-SAD 69 coordinates x	y	NDVI of 09-09-'02 ASTER
groundcover	19 01 17.4	48 24 51	10	70	772197,0	7894785,1	0,083

Filename	Geographic coordinates y	x	estimated field VGC green	total	UTM-SAD 69 coordinates x	y	NDVI of 09-09-'02 ASTER
pasture_groundcover	19 02 51.5	48 25 35.7	60	100	770847,0	7891907,6	0,087

Filename	Geographic coordinates y	x	estimated field VGC green	total	UTM-SAD 69 coordinates x	y	NDVI of 09-09-'02 ASTER
pasture-groundcover_SW	19 04 49.7	48 29 26.1	35	80	764054,8	7888369,8	0,023

Filename	Geographic coordinates y	x	estimated field VGC green	total	UTM-SAD 69 coordinates x	y	NDVI of 09-09-'02 ASTER
groundcover_S	19 02 23.4	48 26 10	5	80	769857,3	7892787,5	0,135

Appendix F: Composites of vegetative ground cover maps

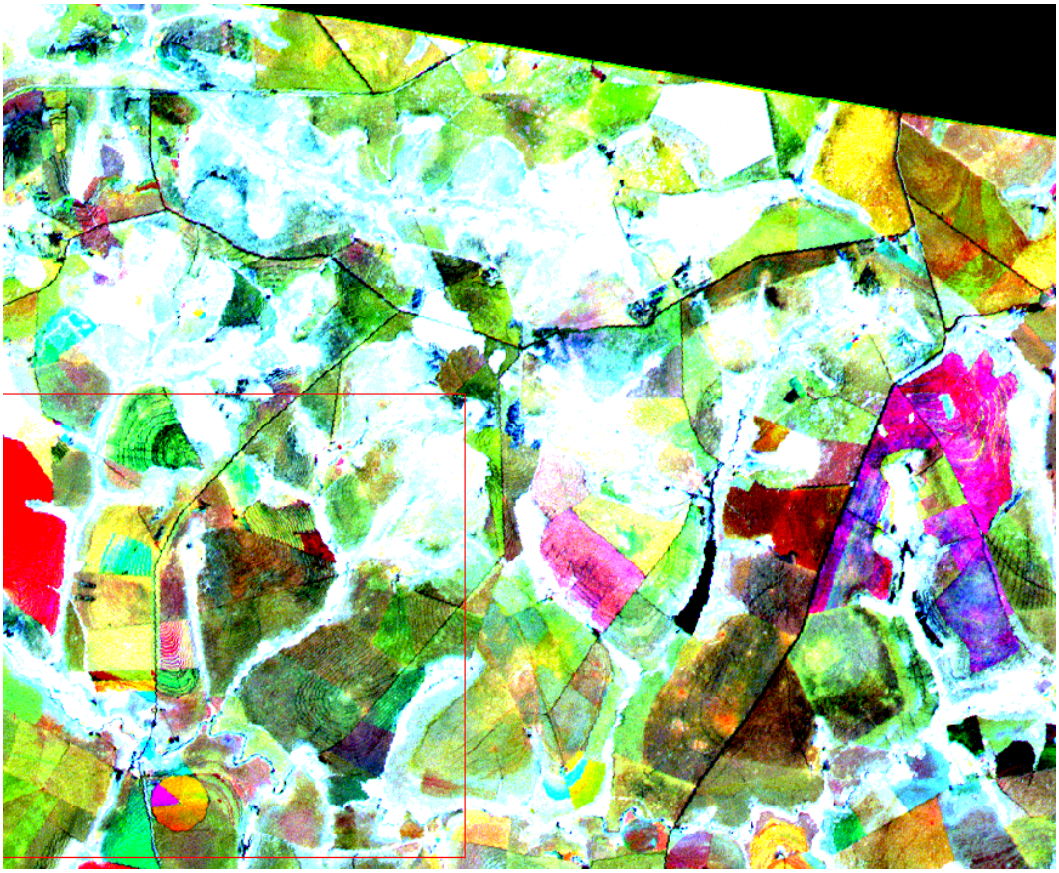

Composite map of three total vegetative ground cover maps in 2003; 4th March 2003 (red), the 23rd of May 2003 (green), 11th August 2003 (blue).

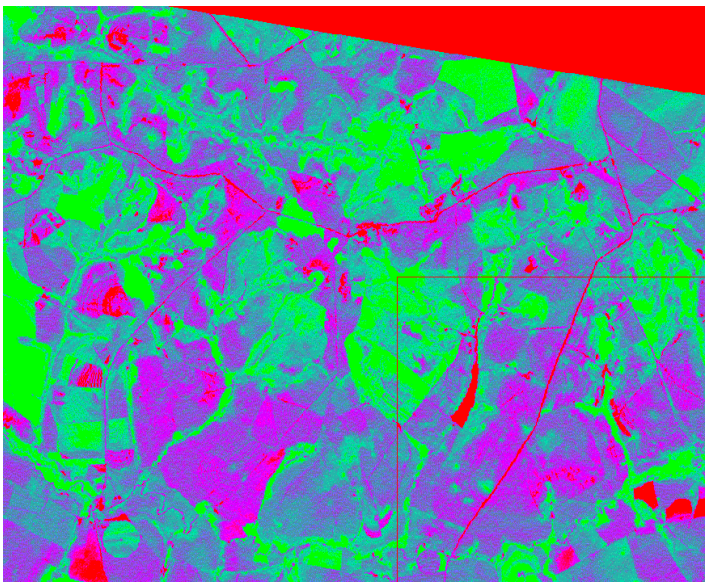

Composite of bare soil (red), green – (green) and yellow (blue) vegetative ground cover maps of the 4th of March 2003, surface reflectance, ASTER level 2B05.

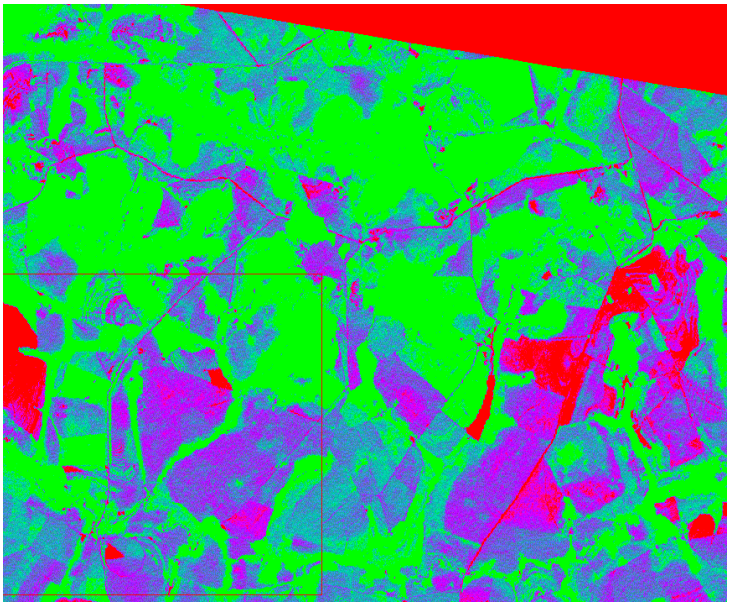

Composite of bare soil (red), green – (green) and yellow (blue) vegetative ground cover maps of the 23rd of May 2003, surface reflectance, ASTER level 2B05.

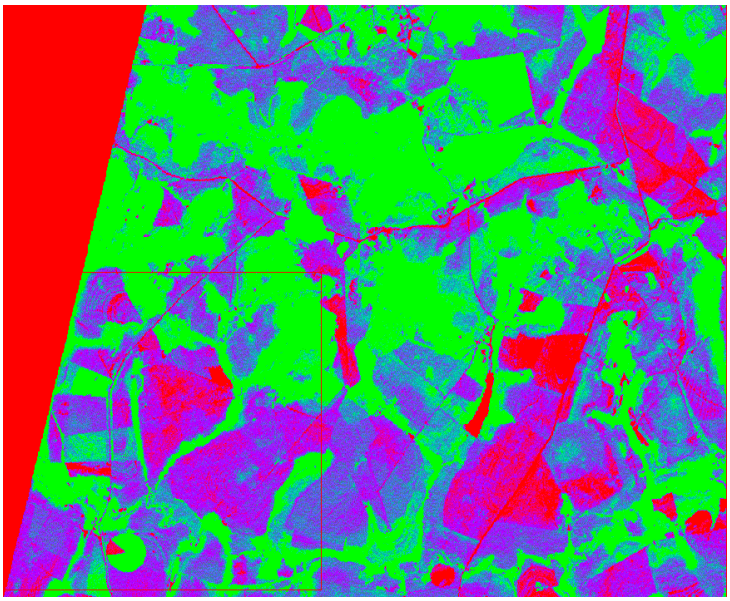

Composite of bare soil (red), green – (green) and yellow (blue) vegetative ground cover maps of the 17th of June 2003, surface reflectance, ASTER level 2B05.

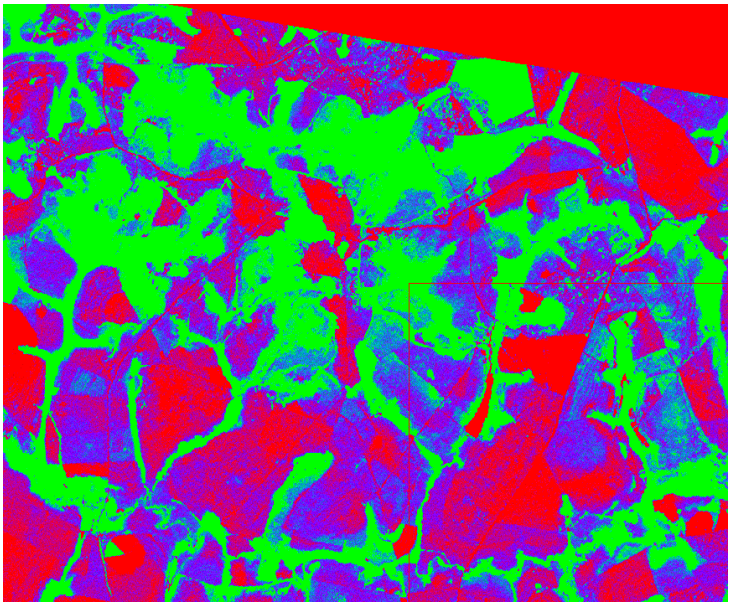

Composite of bare soil (red), green – (green) and yellow (blue) vegetative ground cover maps of the 11th of August 2003, surface reflectance, ASTER level 2B05.

Appendix G: Validation results

field VGC - VGC estimates	040303				250203			
	total	green	yellow	bare soil	total	green	yellow	bare soil
mean:	-3,0	0,6	-3,1	3,0	2,1	5,7	-0,9	-2,1
st.dev.	15,6	16,2	6,9	15,6	13,8	16,3	8,0	13,8
max	30,0	32,0	5,2	30,0	35,0	41,4	10,2	35,0

The mean, standard deviation and maximum values for the differences in vegetative ground cover between 79 field estimates and the ASTER imagery. The 79 points are a subset of all wet season field data that is used to derive the correlation between the total vegetative ground cover and NDVI.

level 1B:	250203_040303	**total**	**green**	**yellow**	**bare soil**
	mean	-4,45	-2,08	-2,37	4,45
	st.dev.	11,20	11,18	3,80	11,20
	min	-100	-100	-22	-100
	max	100	100	15	100
	260201_040303	**total**	**green**	**yellow**	**bare soil**
	mean	-4,66	-3,35	-1,31	4,66
	st.dev.	22,06	24,31	6,77	22,06
	min	-100	-100	-21,71	-100
	max	100	100	15,39	100
level 2B05:	250203_040303	**total**	**green**	**yellow**	**bare soil**
	mean	6,72	7,54	-0,86	-6,68
	st.dev.	11,72	12,15	3,83	11,86
	min	-100	-100	-22,40	-100
	max	100	100	22,40	100
	260201_040303	**total**	**green**	**yellow**	**bare soil**
	mean	7,87	8,33	-0,46	-7,87
	st.dev.	24,75	27,30	6,90	24,75
	min	-100	-100	-22,41	-100
	max	100	100	22,41	100

The ASTER vegetative ground cover maps of the 4th of March 2003 is subtracted from the ASTER vegetative ground cover maps of the 25th of February 2003 and of the ASTER vegetative ground cover maps of the 26th of February 2001. This is calculated for both level 1B (top of the atmosphere radiance) imagery and level 2B05 (surface reflectance) imagery. (Chapter 3..3.2 and 4.3)